Slug, a Cancer-Related Transcription Factor, is Involved in Vascular Smooth Muscle Cell Transdifferentiation Induced by Platelet-Derived Growth Factor-BB During Atherosclerosis

Nahema Ledard, Alexandrine Liboz, Bertrand Blondeau, Mégane Babiak, Célia Moulin, Benjamin Vallin, Isabelle Guillas, Véronique Mateo, Claire Jumeau, Karl Blirando, et al.

ORIGINAL RESEARCH

Slug, a Cancer-Related Transcription Factor, is Involved in Vascular Smooth Muscle Cell Transdifferentiation Induced by Platelet-Derived Growth Factor-BB During Atherosclerosis

Nahéma Ledard, MS;* Alexandrine Liboz, MS;* Bertrand Blondeau, PhD; Mégane Babiak, BS; Célia Moulin, BS; Benjamin Vallin, PhD; Isabelle Guillas, PhD; Véronique Mateo, PhD; Claire Jumeau, PhD; Karl Blirando, PhD; Olivier Meilhac, PhD; Isabelle Limon, PhD;† Martine Glorian, PhD†

***Background*—**Heart attacks and stroke often result from occlusive thrombi following the rupture of vulnerable atherosclerotic plaques. Vascular smooth muscle cells (VSMCs) play a pivotal role in plaque vulnerability because of their switch towards a proinflammatory/macrophage-like phenotype when in the context of atherosclerosis. The prometastatic transcription factor Slug/Snail2 is a critical regulator of cell phenotypic transition. Here, we aimed to investigate the role of Slug in the transdifferentiation process of VSMCs occurring during atherogenesis.

***Methods and Results*—**In rat and human primary aortic smooth muscle cells, Slug protein expression is strongly and rapidly increased by platelet-derived growth factor-BB (PDGF-BB). PDGF-BB increases Slug protein without affecting mRNA levels indicating that this growth factor stabilizes Slug protein. Immunocytochemistry and subcellular fractionation experiments reveal that PDGF-BB triggers a rapid accumulation of Slug in VSMC nuclei. Using pharmacological tools, we show that the PDGF-BB–dependent mechanism of Slug stabilization in VSMCs involves the extracellular signal-regulated kinase 1/2 pathway. Immunohistochemistry experiments on type V and type VI atherosclerotic lesions of human carotids show smooth muscle–specific myosin heavy chain–/Slug-positive cells surrounding the prothrombotic lipid core. In VSMCs, Slug siRNAs inhibit prostaglandin E2 secretion and prevent the inhibition of cholesterol efflux gene expression mediated by PDGF-BB, known to be involved in plaque vulnerability and/or thrombogenicity.

***Conclusions*—**Our results highlight, for the first time, a role of Slug in aortic smooth muscle cell transdifferentiation and enable us to consider Slug as an actor playing a role in the atherosclerotic plaque progression towards a life-threatening phenotype. This also argues for common features between acute cardiovascular events and cancer. **(*J Am Heart Assoc*. 2020;9:e014276. DOI: 10.1161/JAHA.119.014276.)**

Key Words: atherogenesis • inflammation • vascular smooth muscle

Atherosclerosis, the leading cause of death in developed countries, is a chronic inflammatory disease that affects the walls of large and medium arteries. This disease leads to localized wall thickening (atherosclerotic plaques) composed of a cholesterol-rich core surrounded by a fibrous cap. The rupture of vulnerable (ie, unstable) plaques characterized by a large necrotic lipid core, a thin fibrous cap, and an increased number of apoptotic macrophages and vascular smooth muscle cells (VSMCs), leads to the formation of occlusive thrombi likely to cause myocardial infarction and ischemic stroke.[1]

From the Institut de Biologie Paris-Seine (IBPS), Biological Adaptation and Ageing, UMR 8256 (N.L., M.B., C.M., B.V., K.B., I.L., M.G.), INSERM, Saint-Antoine Research Center (A.L., B.B.), National Institute for Health and Medical Research (INSERM), Faculté de Médecine Pitié Salpétrière, UMR-S 1166 ICAN (I.G.), CIMI-Paris INSERM U1135, Faculté de Médecine Sorbonne-Université, Site Pitié-Salpêtrière (V.M.), and INSERM UMR_S 933 (C.J.), Sorbonne Université, Paris, France; Université de La Réunion, Diabète, Athérothrombose, Thérapies, Réunion, Océan Indien (UMR DéTROI U1188) – -CYROI-, Sainte Clotilde, La Réunion (O.M.).

Accompanying Tables S1 through S3 and Figures S1 through S7 are available at https://www.ahajournals.org/doi/suppl/10.1161/JAHA.119.014276

*Dr Ledard and A. Liboz contributed equally to this work as first authors.

†Pr Limon and Dr Glorian contributed equally to this work as last authors.

Correspondence to: Isabelle Limon, PhD, IBPS, CNRS UMR 8256, Sorbonne Université, 7 Quai Saint Bernard, Bâtiment A 5ème étage, Case 256, 75252 Paris Cedex 05, France. Email: isabelle.limon@sorbonne-universite.fr

Received August 12, 2019; accepted September 18, 2019.

Clinical Perspective

What Is New?

- The platelet-derived growth factor-BB–mediated increase of prostaglandin E2 secretion, known to play a key role in atherosclerotic plaque rupture and arterial thrombosis, is a Slug-dependent event in vascular smooth muscle cells.
- The platelet-derived growth factor-BB–mediated downregulation of genes encoding proteins involved in cholesterol efflux (ATP-binding cassette transporters A1 and G1) and in plaque vulnerability/thrombogenicity is a Slug-dependent event in vascular smooth muscle cells.
- Human type V and VI atherosclerotic lesions show smooth muscle–specific myosin heavy chain–/Slug-positive cells surrounding the prothrombotic lipid core.

What Are the Clinical Implications?

- This study reinforces the therapeutic potential of drugs targeting the platelet-derived growth factor/platelet-derived growth factor receptor pathway for the prevention of acute clinical complications of atherosclerosis.
- This study allows for considering any actors of Slug activation pathways as potential therapeutic targets to avoid the atherosclerotic plaque progression towards a life-threatening phenotype.

VSMCs play a pivotal role in atherogenesis when switching to proliferating/migratory/secretory cells involved in the fibrous cap synthesis or by acquiring a macrophage-like phenotype when engulfing oxidized low-density lipoprotein (ox-LDL).[2] Becoming lipid laden cells (ie, foam cells), they contribute to the plaque vulnerability by sustaining the plaque core and secreting inflammatory components rather than the fibrous cap components.[3]

The transcription factor Slug/Snail2 is a critical regulator of cell phenotypic transition. Both members of the Snail family of zinc-finger transcription factors, Snail1 and Snail2/Slug, are known to play a major role in epithelial-mesenchymal transition, which decreases epithelial properties and increases migratory properties, invasiveness and apoptotic resistance of epithelial cells during embryogenesis and cancer metastasis.[4] This particular switch of phenotype shares some similarities with VSMC changes observed during atherosclerosis. In fact, VSMCs: (1) become spindle-shaped cells with migratory protrusions, and (2) undergo a decrease of their differentiation markers including the smooth muscle actin (SMA) and an increase of the level of proteins related to cell migration such as extracellular matrix degrading enzymes. Several in vivo studies also highlight the role of Slug in regulating inflammation.[5–8]

PDGF-BB, one of the growth factors present in every step of atherogenesis,[9] is well known to direct VSMCs towards a migratory/proliferating phenotype.[10] In VSMCs, PDGF-BB also: (1) enhances the expression of multiple proinflammatory molecules including cyclooxygenase-2 (COX-2) and matrix metalloproteinase-9 involved in plaque vulnerability and thrombosis,[11–16] (2) promotes a macrophage-like phenotype,[17] and (3) synergizes with hypercholesterolemia to promote atherosclerosis with unstable plaques.[11]

Snail1 and/or Slug are often targeted by the PDGF signaling pathway to induce such a profound phenotypic switch in other cell types.[18–21]

Here, we highlight, for the first time, the presence of Slug-expressing VSMCs in advanced atherosclerotic lesions of human carotid samples and demonstrate that Slug participates in PDGF-BB–mediated transdifferentiation of VSMCs without triggering any migration against all expectations. Based on these results, we now suggest a causal relationship between Slug expression and plaque vulnerability and thrombogenicity, suggesting a mechanistic link between acute cardiovascular diseases and cancer.[22]

Methods

The authors declare that all supporting data are available within the article (and its online supplementary files).

Compounds, cells, cell media, and their sources are listed in Table S1.

Production of ox-LDL

Human low-density lipoprotein purification and their oxidation were performed as previously described.[23] Human Dil-labeled ox-LDLs (Dil-ox-LDLs) were purchased from Thermofisher Scientific (catalog number L34358).

Cell Cultures

Rat VSMCs were isolated from aorta as previously described.[24] The university's ethic committee approved the experiments on rats, and all animal procedures were conformed to European Directive 2010/63/E. Sources of human primary aortic smooth muscle cells (AoSMCs) and related products are indicated in Table S1.

VSMCs were cultured in DMEM containing 1 g/L glucose, 10% fetal bovine serum, 4 mmol/L L-glutamine, 100 U/mL penicillin, and 100 µg/mL streptomycin (rat VSMC) or smooth muscle growth medium-2 containing 5% fetal bovine serum, penicillin/streptomycin, and smooth muscle cell–specific growth factors and supplements (AoSMCs). All of the experiments were performed at cell passages ranging from 2 to 3 (rat VSMC) or from 5 to 7 (AoSMCs). Treatments are shown in

the figure legends. Sixteen hours before any treatment, cells were made quiescent in a serum-free medium.

Primary cultures of human macrophages were obtained from mononuclear cells isolated from buffy coats of healthy normolipidemic donors, provided by the French Blood Institute (EFS). The isolation procedure and culture conditions were as described in Jumeau et al.[25] All blood donors were volunteers who gave their free and informed written consent, which conformed to the ethical standards of the Declaration of Helsinki. Legal and ethical authorization for the use of collected blood for research was obtained through a national convention between the French National Institute of Health and Medical Research (INSERM) and the EFS (convention number 15EFS012).

Adenovirus Transduction

Adenovirus delivering the hemagglutinin-human Slug cDNA was constructed as previously described.[26] VSMCs were transduced for 24 hours at a multiplicity of infection of 45 in a complete medium before starving them overnight for treatment.

siRNA Transfection

Transfection of siRNA was performed using Lipofectamine RNAiMAX Reagent (Thermo Fisher Scientific) as previously described.[27] Slug siRNA is a mixture of 3 siRNAs (0.3 nmol/L each). The sequences for rat Slug siRNA are shown in Table S2.

RNA Extraction and Polymerase Chain Reaction Reactions

Total RNA was extracted with the ReliaPrep RNA Cell Miniprep System, according to the manufacturer's protocol (Promega). Reverse transcription and quantitative polymerase chain reaction were performed as previously described.[28] The primers used for selective amplification of the cDNAs are shown in Table S2. Melting curve analyses were performed to check reaction specificity. Real-time polymerase chain reaction data are presented as the amount of each target cDNA relative to the amount of cDNA for cyclophilin A (for rat genes) or hypoxanthine-guanine phosphoribosyltransferase (for human genes).

Total Cell Lysates for Western Blot Analysis

Cell lysates were obtained as previously described.[28]

Subcellular Fractionation for Western Blot Analysis

Cells were collected in PBS, centrifuged at 500*g*, and pellets were suspended in 20 mmol/L Tris-HCl pH 7.4, 10 mmol/L NaCl, 3 mmol/L $MgCl_2$ supplemented with proteases and phosphatases inhibitors. NP-40 detergent (0.125%) was added 1 minute later before a 10-minute centrifugation at 3000*g* at 4°C. The supernatant corresponding to the cytoplasmic fraction was collected. Pelleted nuclei were lysed in the cell extraction buffer (Invitrogen) complemented with proteases and phosphatase inhibitors, incubated for 30 minutes on ice and vortexed every 10 minutes before being centrifuged for 30 minutes at 14 000*g* at 4°C. The ultimate supernatant containing nuclear proteins as well as the cytoplasmic fraction were analyzed for their protein content before SDS-PAGE.

Western Blot

Proteins were transferred to a nitrocellulose membrane and Western blot was performed as described.[28] Antibody binding was detected with horseradish peroxidase–conjugated secondary antibodies (Table S3) and enhanced chemiluminescence on a Fujifilm LAS-300 Imager (Fujifilm Medical Systems). We used GAPDH detection to control for equal protein loading and transfer efficiency.

Wound-healing assay was performed as previously described.[27]

Immunocytochemistry

The cells seeded on coverslips were infected with hemagglutinin-tagged human Slug.[26] Serum-starved infected cells were then treated for 1 hour with PDGF-BB (10 ng/mL). Cells were fixed in paraformaldehyde and permeabilized with 0.2% Triton X-100. After blocking in 5% fetal bovine serum, cells were incubated with an anti-hemagglutinin primary antibody and then with an Alexa Fluor 594–conjugated mouse antibody (Table S3). Cell nuclei were visualized using 4′,6′-diamidino-2-phenylindole. The coverslips were mounted in fluorescence mounting medium and examined with a DMi8 S microscope (Leica Microsystems).

Dil-Ox-LDL Uptake

Dil-ox-LDL uptake by VSMCs was examined either with fluorescence microscopy or flow cytometry. For fluorescence microscopy, cells were seeded on collagen-coated coverslips and pretreated with vehicle or PDGF-BB (rat: 10 ng/mL, 6 hours; human: 10 ng/mL, 24 hours) before adding Dil-ox-LDL (rat: 10 μg/mL, 16 hours; human: 10 μg/mL, 4 hours). Cells were fixed and cell nuclei were stained as described above. The coverslips were mounted in fluorescence mounting medium and examined with a DMi8 S microscope. For flow cytometry, the cells were detached with trypsin (0.25% trypsin, 0.02% EDTA), harvested with PBS, centrifuged at 1500*g* for 5 minutes and resuspended in PBS containing 2%

paraformaldehyde. Flow cytometry was performed using an EPICS XL instrument, with Expo32 software (Beckman Coulter). Data were calculated by subtracting the cell autofluorescence from the fluorescence of the treated samples and expressed as mean fluorescence intensity.

Immunohistochemistry

Human carotid endarterectomy samples were collected from patients undergoing surgery at the Centre Cardiologique du Nord (Saint-Denis, France). All patients underwent an interview before surgery and gave their informed consent to use their carotid samples, considered as surgical waste in accordance with French ethical laws (L.1211-3 to L.1211-9) and the INSERM ethics committee. Tissue samples were fixed in 3.7% paraformaldehyde, processed for embedding in paraffin, and 10 µmol/L sections were cut. Pentachrome-stained lesions were classified on the basis of their histological composition and structure in accordance with the report from the American Heart Association Committee on Vascular Lesions.[29] Antigen detections were performed as previously described.[30] Slug, SMA, smooth muscle–specific myosin heavy chain, and CD68 primary antibodies are described in Table S3. Pictures were taken on a Leica DMRB microscope using a Leica QWIN system.

Prostaglandin E2 Assay

Prostaglandin E2 (*PGE2*) secretion was evaluated with an enzyme immunoassay kit from Cayman Chemical SPI-BIO.

Statistical Analysis

All data are presented as the mean±SEM of at least 4 independent experiments. Nonparametric Mann–Whitney tests were performed to compare different experimental conditions. Differences were considered significant if $P<0.05$.

Results

Slug is Expressed in Human Carotid Atherosclerotic Lesions by VSMC Displaying a Macrophage-Like Phenotype

We examined Slug expression on paraffin-embedded cross-sections of human carotids displaying typical type V atherosclerotic lesions according to Stary et al's classification[29] (Figure 1). To this end, we used a human Slug antibody referred to as Slug antibody # 1 in Table S3. The efficacy and specificity of this antibody has been validated in situ on pancreas sections of mice.[31] As shown in Figure 1, brown staining indicated by black arrows, corresponding to Slug-positive cells, clearly appeared at the periphery of the acellular necrotic core (*). Identical results were obtained using another Slug antibody (referred to as Slug antibody # 2, in Table S3) tested for its efficacy and selectivity on sections of invasive ductal carcinoma of breast (data not shown). Slug signal was not detected in SMA-positive VSMCs, whether they are localized in the medial layer or in the fibrous cap (Figure 1). However, Slug labeling partially merged that of: (1) CD68, a macrophage marker described to be also expressed by transdifferentiated VSMCs that have adopted a foam phenotype,[32,33] and (2) smooth muscle–specific myosin heavy chain, a specific VSMC marker.[34] Similar results are observed on type VI atherosclerotic lesions (ie, ruptured type V lesion; Figure S1).

Primary cultures of human AoSMCs display a clear basal expression of the Slug mRNA (Figure 2A, left) and protein (Figure 2A, right), whereas Slug transcript and protein were neither detectable in primary culture of human macrophages (Figure 2A, left and right) activated or not by proinflammatory cytokines (Figure 2B). Conversely, Snail1 mRNA is well detected in AoSMCs and primary cultures of human macrophages (Figure S2). These results demonstrate that Slug-positive cells within human culprit plaques are chiefly transdifferentiated VSMCs that have adopted a macrophage-like phenotype.

Slug is Stabilized by PDGF-BB in AoSMCs

The absence of the Slug protein in medial differentiated VSMCs (Figure 1) suggests that Slug protein level is increased in Slug-positive cells in response to growth factors or inflammatory molecules secreted within the neointima. We investigated the ability of PDGF-BB to enhance Slug expression in AoSMCs since: (1) as previously mentioned, PDGF-BB is a key actor of multiple aspects of VSMC transdifferentiation, and (2) some PDGF family members have been demonstrated to trigger Snail1 and Slug expression in other cell types.[18–21] As shown in Figure 3A, Slug protein level was significantly increased by 4.14-fold (n=4, P=0.0286) upon treatment with 10 ng/mL of PDGF-BB as soon as 2 hours (lane 3 versus lane 1) and declined progressively. The PDGF-BB–mediated increase of Slug does not involve *SLUG* gene upregulation since Slug mRNA level remains unchanged upon PDGF-BB treatment up to 6 hours (Figure 3B). Consistently with Snail and Slug proteins being highly unstable and degraded by the proteasome, treatment with the proteasome inhibitor MG132 (10 µmol/L, 1–6 hours) triggers a time-dependent enhancement of Slug protein (Figure 3C upper). When PDGF-BB is added during the MG132 treatment, it only slightly increases MG132 effect on Slug protein level (Figure 3C, lower). Altogether, these results strongly suggest that PDGF-BB stabilizes Slug protein in VSMCs.

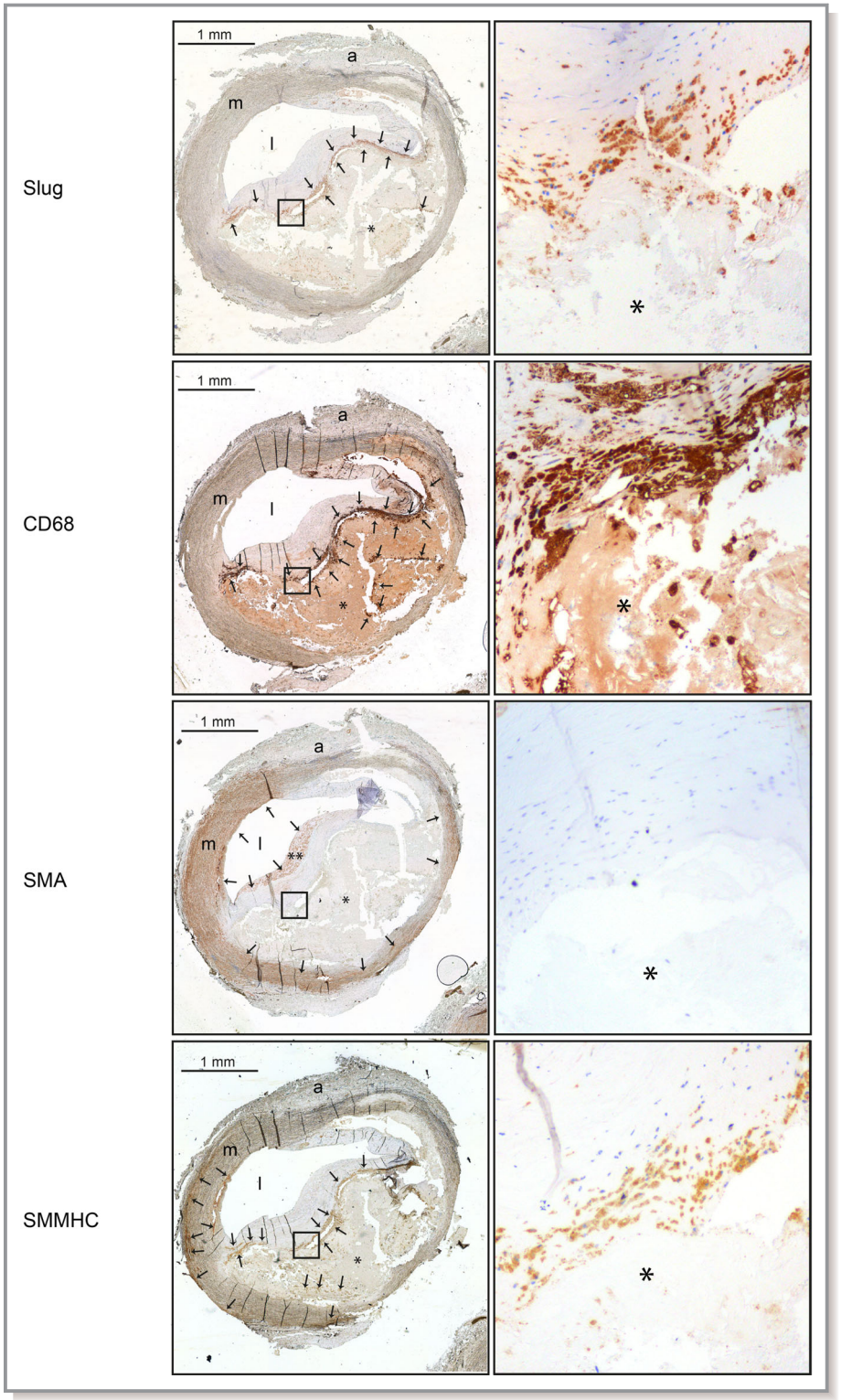

Figure 1. Slug is chiefly expressed by vascular smooth muscle cells that adopted a macrophage-like phenotype in the neointima of type V atherosclerotic lesions of human carotid arteries. Serial sections of a representative human type V atherosclerotic lesion obtained from a carotid endarterectomy sample counterstained with hematoxylin and immunolabeled with an anti-Slug, an anti-CD68, an anti–smooth muscle actin (SMA), or an anti–smooth muscle–specific myosin heavy chain (SMMHC). Images of right panels are obtained at a magnification of × 10. Proteins of interest appearing in brown are indicated by black arrows. The images are representative of serial sections from 4 different patients. a indicates adventitia, l, lumen; m, media. *Lipid core. **Fibrous cap.

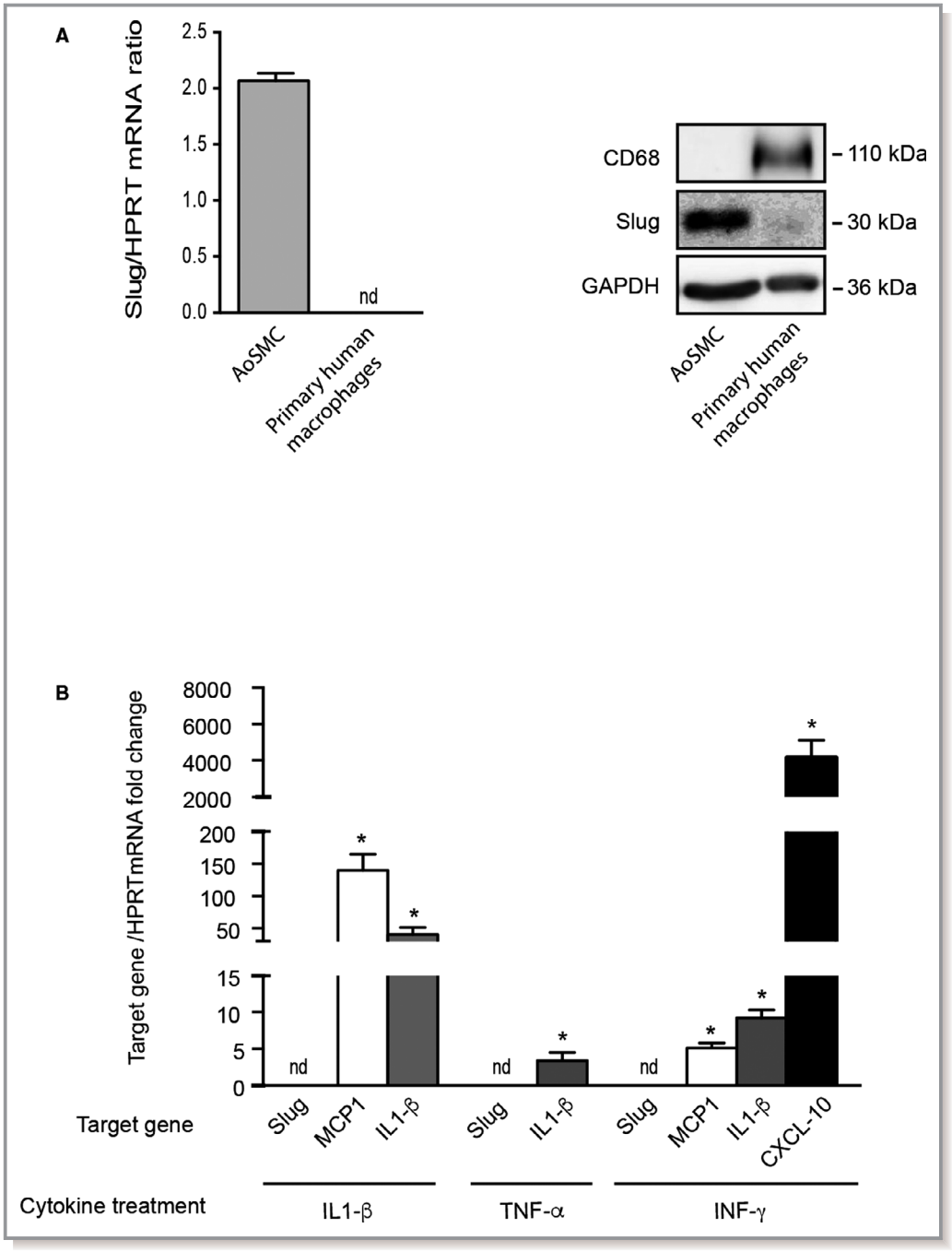

Figure 2. Slug is not detected in primary human macrophages. **A**, Left panel: Slug transcripts expression in primary human macrophages and primary human aortic smooth muscle cells (AoSMCs). Polymerase chain reaction (PCR) results are expressed as the mean relative ratio (target gene/reference gene [hypoxanthine-guanine phosphoribosyltransferase (HPRT)]) obtained from 4 experiments. Right panel: Western blot showing Slug and CD68 protein expression in primary human macrophages and AoSMCs. GAPDH is a loading control. **B**, Transcripts expression in primary human macrophages treated or not during 24 hours with interleukin 1-β (IL1-β; 10 ng/mL), tumor necrosis factor α (TNF-α; 25 ng/mL), or interferon γ (INF-γ; 25 ng/mL). PCR results normalized relative to HPRT are the mean of 4 experiments and are expressed as fold change relative to vehicle-treated macrophages. CXCL-10 indicates C-X-C motif chemokine 1; MCP1, monocyte chemoattractant protein 1; nd, nondetectable. *P<0.05.

To decipher the molecular mechanism(s) involved in PDGF-BB–mediated increase of Slug in VSMCs, we used primary culture of rat aortic VSMCs expressing the human form of Slug tagged with hemagglutinin. In VSMCs infected by a virus coexpressing the human hemagglutinin-Slug and the green fluorescent protein, Slug expression, barely detectable

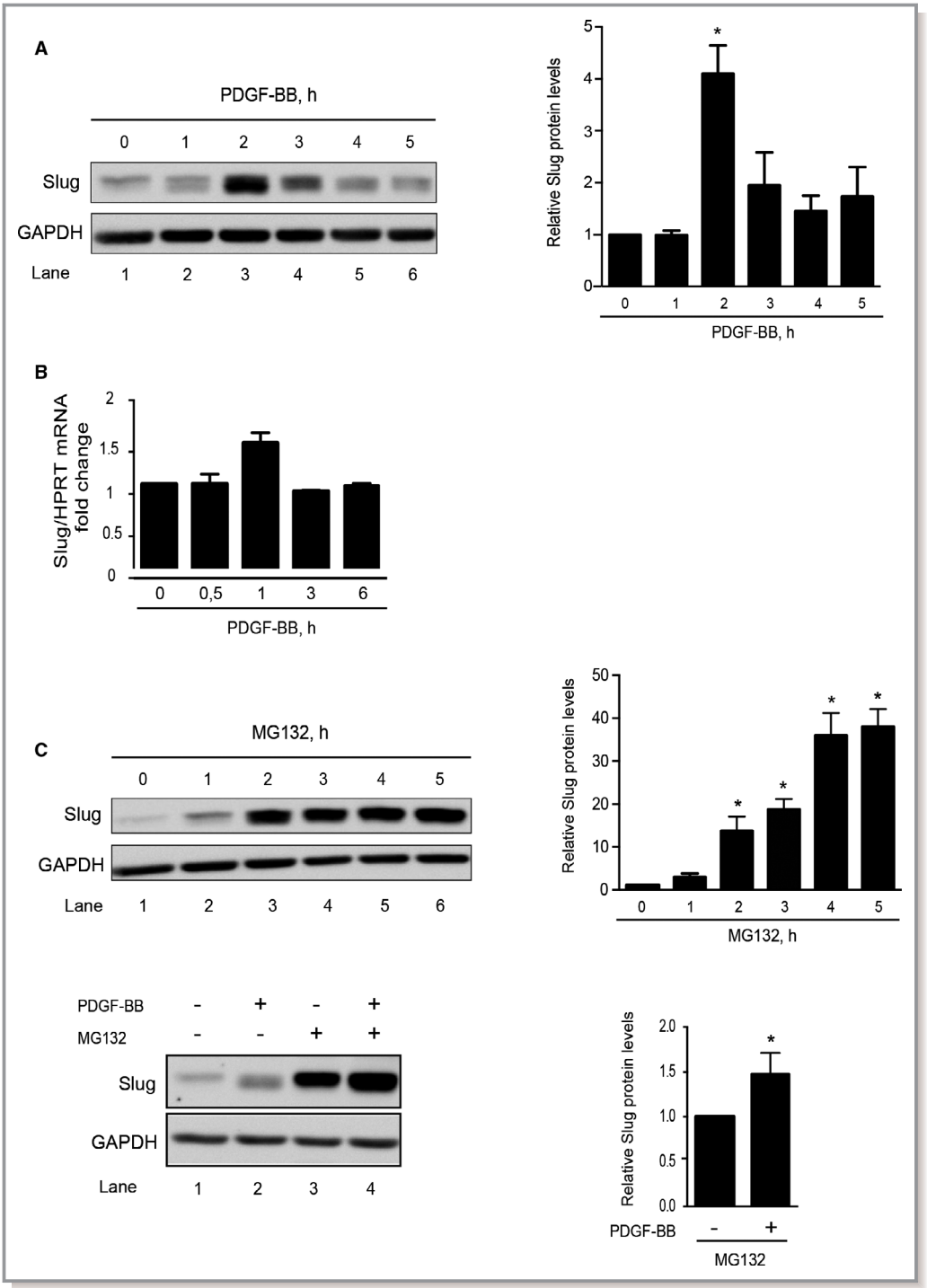

Figure 3. Slug is an unstable protein in human vascular smooth muscle cells (aortic smooth muscle cells [AoSMCs]), whose level is increased by platelet-derived growth factor-BB (PDGF-BB). **A**, Left panel: Western blot representative of 4 experiments showing the time-dependent effect of PDGF-BB (10 ng/mL) on Slug expression. GAPDH is a loading control. **A**, Right panel: quantification of bands intensity. **B**, Slug transcripts expression relative to the length of time of a 10 ng/mL PDGF-BB treatment. Data represent mean±SEM of 4 independent experiments. Results are expressed as fold over control and are normalized relative to hypoxanthine-guanine phosphoribosyltransferase (HPRT). **C**, Left panel: Western blot representative of 4 experiments showing the time-dependent effect of 10 μmol/L MG132 on Slug level (upper) and the effect of 4-hour MG132 (10 μmol/L) on 2-hour PDGF-BB (10 ng/mL)–treated cells (lower); Right panel: quantification of the Western blot bands intensity. For quantification of bands intensity, results (**A** and **C** right panels) are normalized relative to GAPDH and expressed as the mean fold over untreated AoSMCs obtained from 4 independent experiments *P<0.05.

without any treatment, significantly increases as soon as 10 minutes following PDGF-BB treatment (Figure 4A, upper, lane 2 versus 1) and reaches a maximal expression within an hour (Figure 4A, upper, lane 4; see Figure S3A, upper, for densitometry analysis). It should be noted that PDGF-BB does not promote any change of expression of the green fluorescent protein that is expressed in the virus under the control of the same promoter as hemagglutinin-Slug (data not shown). When infected cells are treated with increasing doses of PDGF-BB during 1 hour, the positive effect on hemagglutinin-Slug expression starts at 1 ng/mL and reaches a maximum effect at 10 ng/mL (Figure 4A, lower; see Figure S3A, lower, for densitometry analysis). Treating VSMCs with the proteasome inhibitor MG132 (10 μmol/L, 1–6 hours, Figure 4B, upper; see Figure S3B, upper, for densitometry analysis) triggers a time-dependent increase of hemagglutinin-Slug similar to the effect of MG132 on endogenous Slug in human AoSMCs (Figure 3C). Pretreating VSMCs with MG132 (10 μmol/L, 4 hours) before adding PDGF-BB (10 ng/mL, 1 hour) did not increase the PDGF-BB effect on hemagglutinin-Slug protein level (Figure 4B, lower; see Figure S3B, lower, for densitometry analysis). PDGF-BB treatment increases Slug predominantly in the nucleus, as shown by immunocytofluorescence experiments (Figure 4C) and by cell extract fractionation approach discriminating cytosolic and nuclear proteins such as GAPDH and histone deacetylase 1, respectively (Figure 4D). Altogether, these results strongly suggest that, in VSMCs, the PDGF-BB stabilizes Slug expression by inhibiting its proteasome-mediated degradation and by promoting Slug translocation towards the nucleus.

In epithelial cells, the ubiquitination as well as the proteasome-mediated degradation of the Snail family members involve glycogen synthase kinase-3β (GSK3β)–dependent phosphorylations. Conversely, the increase of Slug level within the cell in response to inflammatory mediators, hypoxia, or growth factors occurs through the inhibition of GSK3β activity.[35–38] It has been shown that in rat VSMCs expressing hemagglutinin-Slug, PDGF-BB treatment rapidly triggers GSK3β phosphorylation and therefore the inhibition of GSK3β activity through the PI3kinase-Akt pathway.[39] We then treated infected VSMCs with PDGF-BB and the PI3kinase inhibitor LY2940002 (25 μmol/L) and monitored Slug level (Figure 5A, left panel, and 5C); the phosphorylation status of Akt and GSK3β (Ser9) were measured as positive controls of LY2940002 treatment. Surprisingly, the positive effect of PDGF-BB on Slug is slightly increased by LY2940002 (lane 4 versus lane 3). Consistently, the level of Slug protein remains undetectable in cells treated by CHIR99021, a selective inhibitor of GSK3β. As expected, MG132 used as a positive control strongly raises the level of Slug (Figure 5A, right panel, lane 3) and this level was potentiated when adding both CHIR99021 and MG132 (Figure 5A, right panel, lane 4). As expected, LY2940002 inhibits the PDGF-BB–induced phosphorylation of both Akt and GSK3β, albeit to a lesser extent for GSK3β (Figure 5A, left panel, lane 4 versus 3, and 5C).

Site directed mutagenesis established serine 87 and 104 of Slug as extracellular signal-regulated kinase (ERK) phosphorylation motifs.[40] When experiments of similar design were performed with 2 pharmacologic inhibitors of the ERK1/2 pathway (U0126 and PD98059, Figure 5B and 5C), the increase of Slug level obtained by PDGF-BB treatment was inhibited as compared with cells treated with PDGF-BB alone (lane 5 and 6 versus 4). As expected, the phosphorylation of ERK1/2 is reduced, whereas total level of ERK remains stable (lane 2 and 3 versus 1). Altogether, these results demonstrate that PDGF-BB stabilizes Slug through the mitogen-activated protein kinase/ERK1/2 cascade and rule out any involvement of the PI3kinase/Akt/GSK3β pathway.

Slug is Involved in the PDGF-BB–Induced VSMC Transition Towards an Inflammatory Phenotype

Slug has been shown to be particularly involved in cell migration during embryonic development and tumor progression.[41] We next determined whether VSMC migration and/or proliferation induced by the PDGF-BB is a Slug-dependent phenomenon. To this end, we took advantage of the wound-healing assay and measured the recolonization capacity of PDGF-BB–treated VSMCs transfected with 3 interfering RNA duplexes (Slug siRNA). Slug siRNA mixture's efficiency and specificity (Figure S4) are attested by a strong inhibition of the expression of Slug mRNA (85% versus control siRNA-transfected cells, P=0.0012) with no effect on Snail1 and Snail3 transcripts expression. As shown in Figure 6, PDGF-BB (10 ng/mL) induced a near-complete recolonization of the experimental wound within 48 hours by the control siRNA-transfected cells. Interestingly, Slug inhibition did not have any impact. The same observations could be made when the wound healing assay was stopped earlier (15 hours post-injury, Figure 6), ie, when cells migrate without proliferating upon PDGF-BB treatment.[42] The lack of effect of Slug siRNA on the PDGF-BB–induced recolonization at 15 and 48 hours post-injury clearly demonstrates that the Slug transcription factor is neither involved in the proliferation nor in the migration of rat VSMCs.

Several studies have highlighted the role of Slug in regulating inflammatory gene expression possibly by interacting with specific E-box elements present in their promoters.[5–8] In atherosclerotic plaques, the secretion of the proinflammatory PGE2, one of the products of COX-2, activates matrix metalloproteinase secretion from macrophages, making the plaque vulnerable[14,15] and enhancing platelet thrombogenicity.[16] In VSMCs, the COX-2 gene is

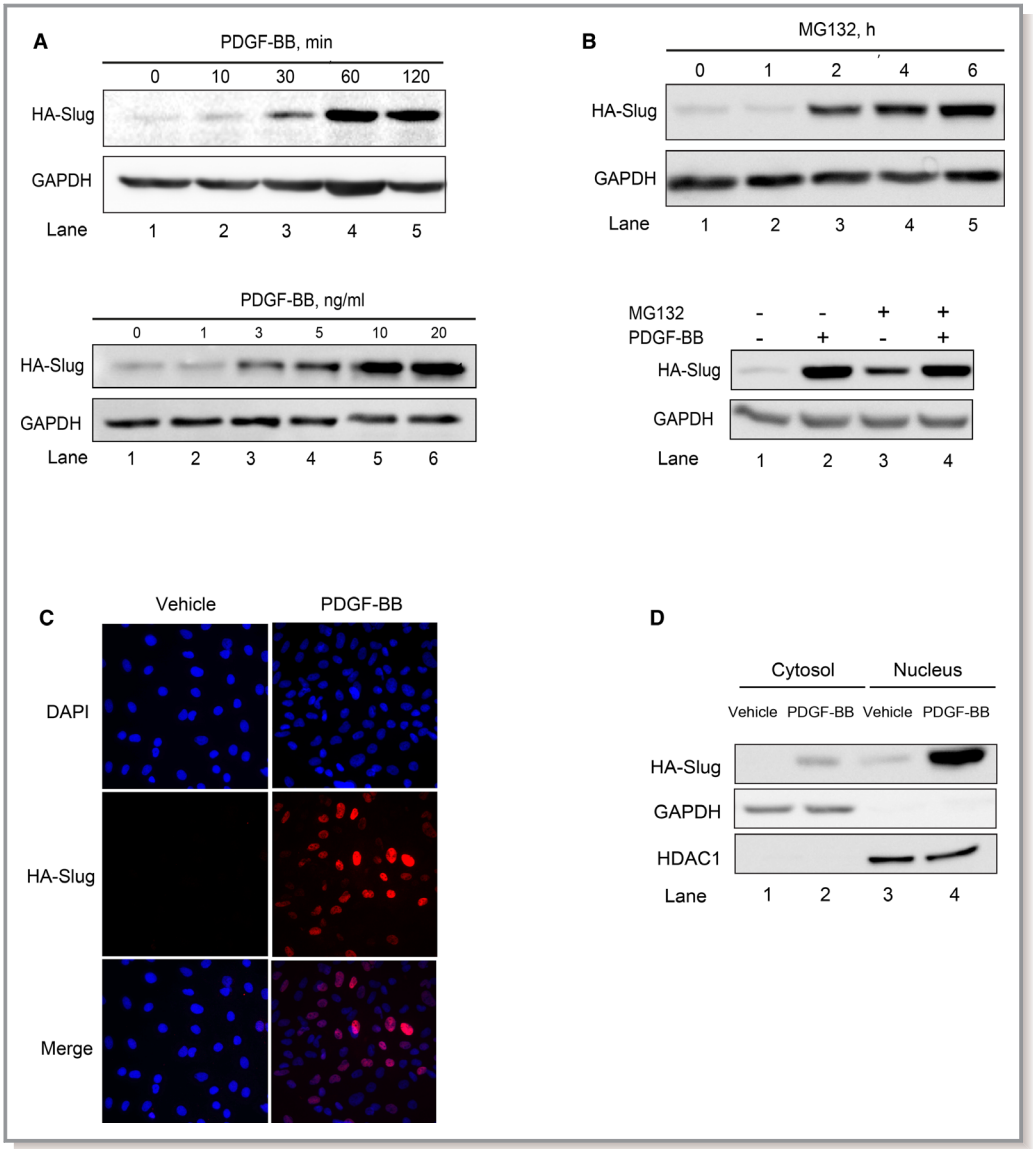

Figure 4. Platelet-derived growth factor-BB (PDGF-BB) stabilizes Slug in the nuclei of rat vascular smooth muscle cells (VSMCs). **A** through **D**, Slug protein expression in rat VSMCs infected with an adenovirus delivering hemagglutinin-human Slug (HA-Slug) detected by an anti-hemagglutinin. GAPDH is a loading control. All images are representative of 4 independent experiments. **A**, Time- (upper) and dose-dependent (lower) effect of PDGF-BB. The concentration of PDGF-BB used for the kinetic (upper) is 10 ng/mL. The length of time of the treatments performed with increasing concentrations of PDGF-BB is 1 hour. **B**, Time-dependent effect of 10 µmol/L of MG132 on Slug-hemagglutinin expression in infected rat VSMCs. **C**, Snapshots of Slug immunostaining on paraformaldehyde-fixed 4′,6′-diamidino-2-phenylindole (DAPI)–stained VSMCs treated with vehicle or PDGF-BB (10 ng/mL, 1 hour). Immunolabelings were analyzed by fluorescence microscopy (×40). Images shown are representative of 4 independent experiments. **D**, Slug, GAPDH, and histone deacetylase 1 (HDAC1) expression in cytosolic and nuclear fractions from cells treated with vehicle or PDGF-BB (10 ng/mL, 1 hour). Densitometry analyses of Western blots are given in Figure S3.

strongly induced by PDGF-BB[43] and is upregulated in oral keratinocytes through a Snail1-dependent mechanism.[44] In addition, COX-2 gene activation by PDGF-BB in VSMCs translates into a significant rise in COX-2 protein[12] and secreted PGE2 levels (around 10-fold as compared with control, P=0.0286; Figure S5). Based on that, we thought of determining whether Slug could play a role in the expression of COX-2 and the related PGE2 secretion induced by PDGF-BB. As shown in Figure 7, Slug siRNA significantly reduced the increase of COX-2 transcripts (Figure 7A), COX-2 proteins (Figure 7B), and secreted PGE2 molecules (Figure 7C) induced by PDGF-BB (10 ng/mL) as compared with control

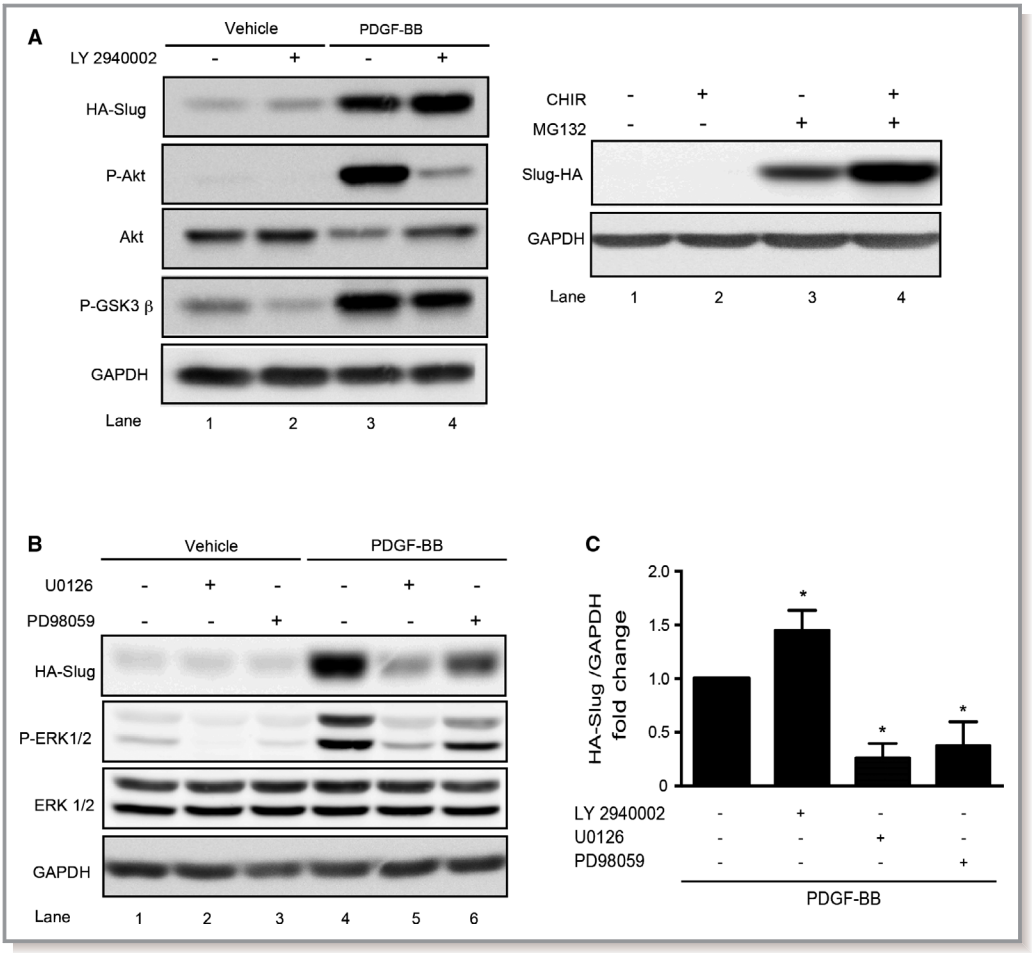

Figure 5. Platelet-derived growth factor-BB (PDGF-BB) stabilizes Slug through the extracellular signal-regulated kinase 1/2 (ERK1/2) pathway in vascular smooth muscle cells. Cells were infected with an adenovirus delivering hemagglutinin-human Slug (HA-Slug). **A**, Left panel: representative Western blot showing Slug, GAPDH, and total Akt expression as well as the phosphorylation of Akt and GSK3β on Ser473 and Ser9, respectively, in cells preincubated (or not) with the PI3kinase/Akt inhibitor LY2940002 (25 μmol/L) during 1 hour and treated for an additional hour with PDGF-BB (10 ng/mL) or vehicle. **A**, Right panel: representative Western blot showing Slug expression in cells treated for 6 hours with or without the glycogen synthase kinase-3β (GSK3β) inhibitor CHIR99021 (3 μmol/L) and/or MG132 (10 μmol/L). **B**, Representative Western blot showing Slug, GAPDH, total ERK1/2, and P-ERK1/2 expressions in cells preincubated with the ERK1/2 inhibitors U0126 (10 μmol/L) and PD98059 (15 μmol/L) for 1 hour and/or treated for 1 hour with PDGF-BB (10 ng/mL) or vehicle. **C**, Densitometry analysis of Western blots from 4 independent experiments showing HA-slug relative to GAPDH expression in PDGF-BB–treated cells in the presence of LY2940002, U0126, or PD98059. PDGF-BB+LY2940002, U0126, or PD98059 vs PDGF-BB alone, **P*<0.05.

siRNA-transfected cells. When experiments of similar design were performed in the presence of U0126 and/or PD98059 (Figure 7D through 7F), the induction of COX-2 gene, protein, and PGE2 secretion was reduced as compared with that observed in cells treated with PDGF-BB alone. The inhibition of COX-2 transcripts, protein, and PGE2 in PDGF-BB–treated VSMCs transfected by siCtrl was of ≈55%, 55%, and 47%, respectively, to that of VSMCs transfected with SLUG siRNA, and that in PDGF-BB–treated VSMCs processed with U0126 or PD98059 was of ≈60%, ≈70% and ≈75%, or ≈55% and 45%, respectively. These results demonstrate that the Slug transcription factor is involved in the PDGF-BB–induced transitions of VSMCs towards an inflammatory state, which favors atherosclerotic plaque instability.

Slug is Involved in the PDGF-BB–Mediated Downregulation of Genes Involved in Cholesterol Efflux

As mentioned in the introduction, PDGF-BB allows VSMCs to become foam cells.[17] Consistently, PDGF-BB triggers DiI-ox-LDL uptake in rat (Figure 8A) and human VSMCs (Figure S6),

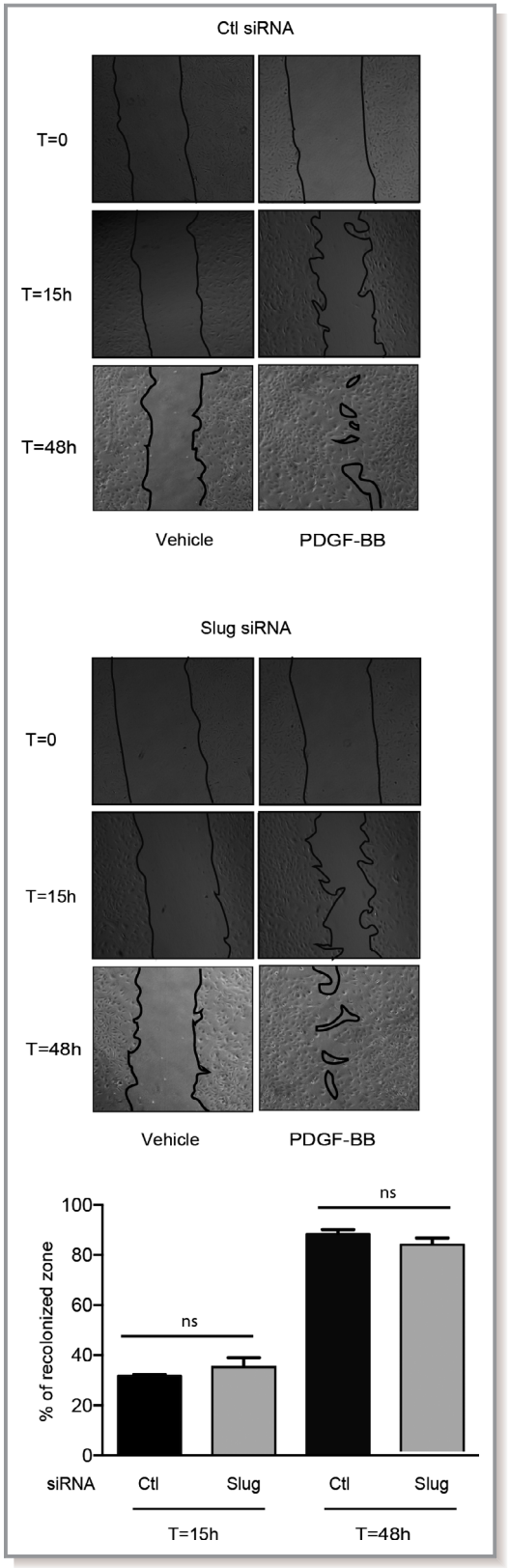

Figure 6. The downregulation of Slug has no effect on platelet-derived growth factor-BB (PDGF-BB)–mediated migration and proliferation. Wound healing assay on serum-starved vascular smooth muscle cells transfected by control (Ctl) or Slug siRNA and treated with vehicle or 10 ng/mL PDGF-BB during 15 or 48 hours. Upper and middle panels: snapshots of a representative wound healing assay (obtained by phase contrast microscopy, objective ×4) at time 0 (T0h), 15 (T15h), and 48 hours (T48h). Lower panel: quantification of the recolonized zone. The recolonized zone is the mean±SEM of 3 independent experiments and is expressed as the percentage of recolonization in the presence of PDGF-BB at T15h or T48h over T0h. ns indicates not significant.

but this effect is Slug independent (Figure 8A). Indeed, the PDGF-BB–mediated uptake of Dil-ox-LDLs is similar whether in Slug siRNA or control-transfected cells as evidenced in fluorescence microscopy (upper) and flow cytometry (lower) data. However, the maintenance of a foam phenotype also results from impaired cholesterol efflux by ATP-binding cassette transporter A1 (ABCA1) and G1 (ABCG1).[45] The PDGF-BB suppresses ABCA1 gene and protein expression in human VSMCs (data not shown and reference 46) and similar results were found in rat VSMCs (Figure 8B). Knocking down the expression of Slug significantly inhibits PDGF-BB–mediated and G1 gene inhibition (Figure 8B). Of note, Slug siRNA transfection significantly increases basal expression of both genes. Altogether, this last set of experiments is in favor of an important role of Slug in the deleterious effect of PDGF-BB on cholesterol efflux.

Discussion

The increase of Slug upon PDGF-BB treatment in VSMCs was consistent with what was previously observed for Snail1 and Snail2 in mesenchymal, endothelial, and prostate cancer cells.[18–21] Experiments demonstrating that PDGF-BB increases Slug protein without affecting mRNA levels indicate that this growth factor stabilizes Slug protein. The PDGF-BB–dependent mechanism of Slug stabilization in VSMCs does not involve the inhibition of GSK3β activity like in most epithelial cell types,[36–38] but the activation of the ERK1/2 pathway (Figure 5). As for Snail1 in breast cancer cells and prostate cancer,[47] ERK1- and/or 2-mediated phosphorylation of Slug or an intermediary protein may protect Slug from the ubiquitination and subsequent proteasome degradation, leading to its nuclear accumulation.

Our in vitro results rule out any involvement of Slug in the migration and proliferation of VSMCs induced by the PDGF-BB. This seems to contradict the results obtained by Coll-Bonfill et al,[48] which demonstrate that Slug participates in the serum-induced proliferation/migration of human pulmonary artery SMCs in primary cultures. However, in this study, Slug

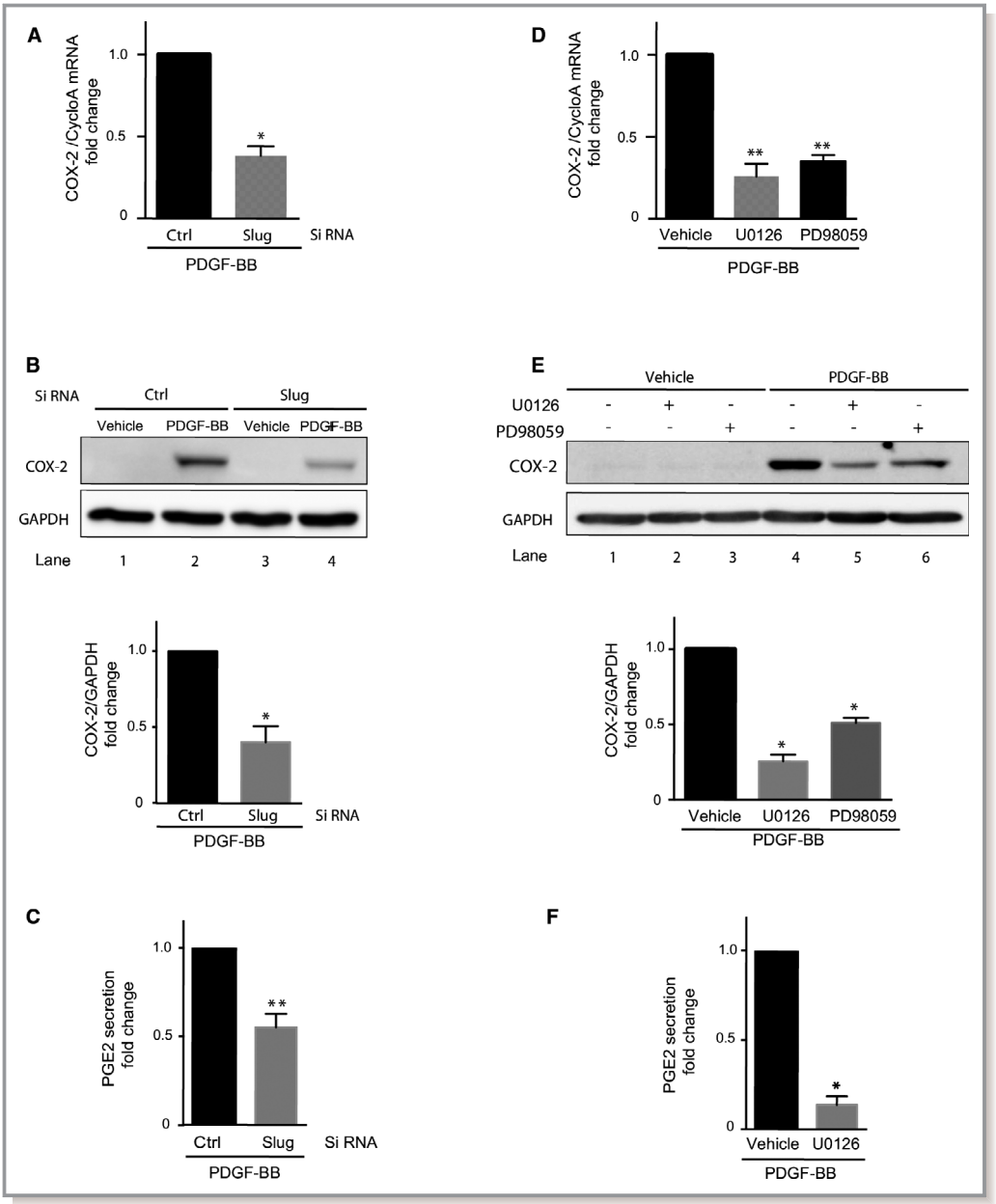

Figure 7. Slug is involved in vascular smooth muscle cell (VSMC) transition towards an inflammatory phenotype. Cyclooxygenase-2 (COX-2) mRNA level (real-time quantitative polymerase chain reaction [RT-qPCR], **A** and **D**) and protein expression (Western blots, **B** and **E**) in VSMCs treated with vehicle or 10 ng/mL of PDGF-BB for 1 hour (RT-qPCR) to 2 hours (Western blot). Cells were either transfected by control (ctrl) or Slug siRNA (**A** and **B**) or preincubated for 1 hour with 10 μmol/L U0126 or 15 μmol/L PD98059, both extracellular signal-regulated kinase (ERK1/2) inhibitors, or vehicle (**D** and **E**). **A** and **D**, Polymerase chain reaction results normalized relative to cyclophilin A (cycloA) are the mean of 4 experiments and are expressed as fold change relative to platelet-derived growth factor-BB (PDGF-BB)–treated VSMCs. **B** and **E**, Upper panels: Western blots are representative images of 3 experiments. GAPDH was used as a loading control. **B** and **E**, Lower panels: quantification of band intensity. Results are normalized relative to GAPDH and expressed as the mean fold over PDGF-BB–treated VSMCs obtained from 4 independent experiments. **C** and **F**, Prostaglandin E2 (PGE2) concentrations in cell supernatants were determined in VSMCs treated with vehicle or 10 ng/mL of PDGF-BB for 9 hours. Cells were either transfected by ctrl or Slug siRNA (**C**) or preincubated for 1 hour with 10 μmol/L of U0126 or vehicle (**F**). Results are expressed as fold change relative to PDGF-BB–treated VSMCs from 4 to 6 independent experiments. *P<0.05; **P<0.005.

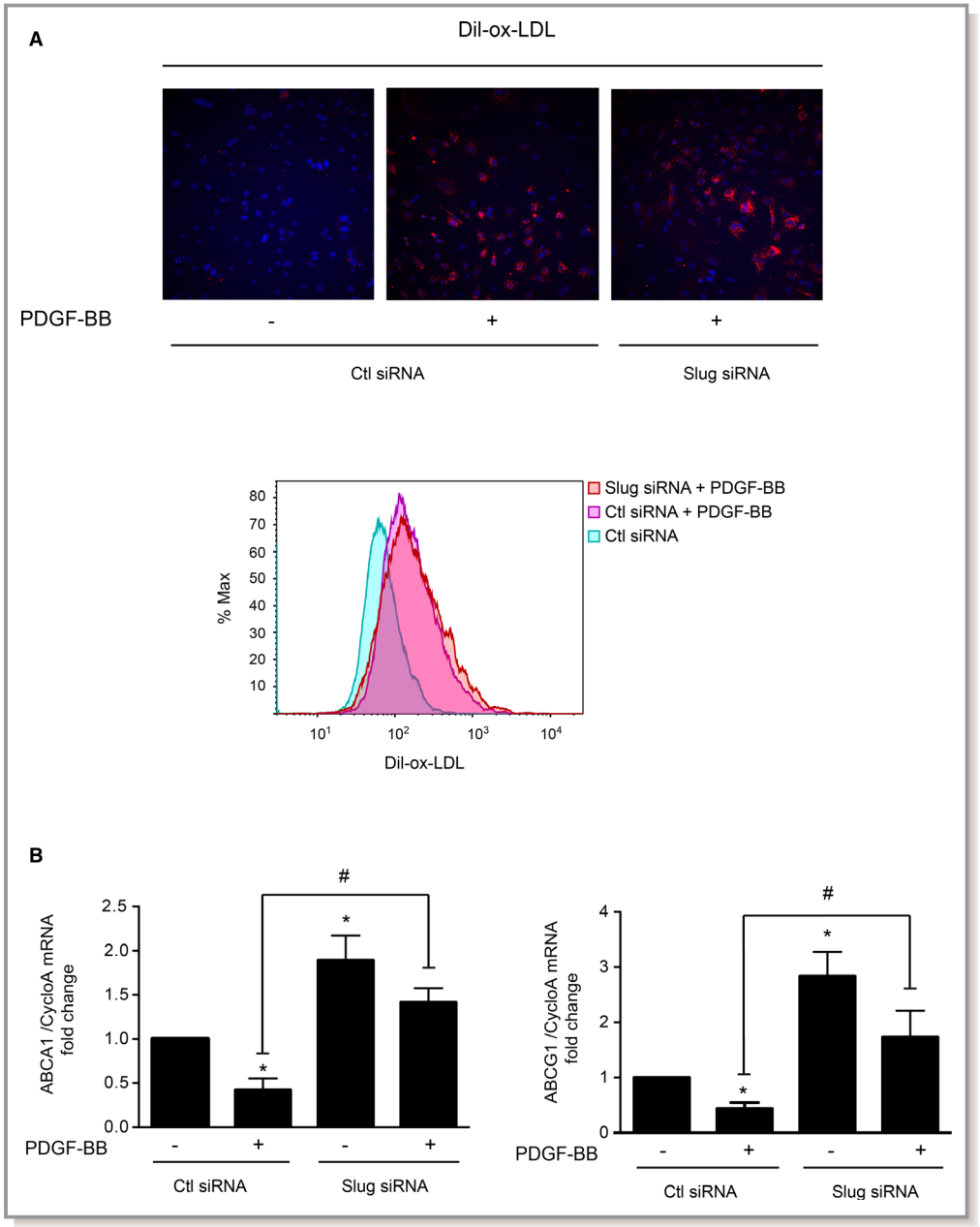

Figure 8. Slug is involved in the platelet-derived growth factor-BB (PDGF-BB)–mediated downregulation of genes involved in cholesterol efflux. DiI-labeled oxidized low-density lipoprotein (DiI-ox-LDL, 10 μg/mL, 16 hours) uptake by control- (Ctl) or Slug-siRNA transfected rat vascular smooth muscle cells (VSMCs) pretreated with vehicle or PDGF-BB (10 ng/mL, 6 hours). Cells are fixed with paraformaldehyde and 4′,6′-diamidino-2-phenylindole stained for analysis by fluorescence microscopy (×20, **A**, upper panel) or directly analyzed by flow cytometry (**A**, lower panel). **A**, Upper panel: snapshots representative of 3 independent experiments where 6 different fields per condition were examined. **A**, Lower panel: flow cytometry histogram representative of 3 independent experiments. **B**, Transcripts expression of ATP-binding cassette subfamily A1 (ABCA1) and G1 (ABCG1). Polymerase chain reaction results are expressed as the mean relative ratio (target gene/reference gene cyclophilin A [CycloA]) obtained from 4 experiments vs Ctl siRNA transfected cells: *P<0.05; vs Ctl siRNA-transfected cells treated with PDGF-BB: $^{\#}P$<0.05.

knockdown pulmonary artery SMCs were tested for their migration and proliferation capacity in a growth medium including several indefinite growth factors, making comparison difficult. In addition, pulmonary artery SMCs have often been shown to display a unique behavior and repertoire of proteins, attesting for a specialization of VSMCs along the arterial tree.[49]

Consistently with the PDGF-BB–positive effect on the foam phenotype of VSMCs,[17] this growth factor increases ox-LDL entry (Figure 8A and Figure S6) and decreases the expression of genes encoding proteins involved in cholesterol efflux (ABCA1 and ABCG1, Figure 8B and 46). The efflux of cholesterol is likely to be regulated by Slug since Slug knockdown not only prevents the PDGF-BB inhibitory effect on these 2 genes but also increases their basal expression. Consistently, we found SNAI2 MA0745.1 motifs (JASPAR CORE 2018 vertebrates library) within the promoters of human and mouse ABCA1 and ABCG1 genes by an extensive in silico analysis using the FindM software (The Eukaryotic Promoter Database) and selecting "best matches" or "all matches" sequences.

By modulating cholesterol homeostasis, Slug may be a key transcription factor to the PDGF-BB–mediated plaque vulnerability[11,50] and apoptotic effects[45] involved in plaque thrombogenicity.[51]

Our in vitro results also demonstrate that in VSMCs, Slug is involved in the PDGF-BB–induced expression of COX-2 and related PGE2 secretion, also making Slug a protagonist of the PDGF-BB–induced VSMC phenotypic transition towards an inflammatory phenotype. The role played by Slug in VSMC phenotypic transition is consistent with the fact that Slug is a critical regulator of cell fate by playing determinant roles in epithelial-mesenchymal transition,[4] endothelial-mesenchymal transition,[52] and, more broadly, cell identity.[53]

Although the precise Slug-dependent molecular mechanism by which PDGF-BB increases the expression of the COX-2 gene remains to be explored, it is probably an indirect process such as the one regulating the *VIMENTIN* gene in cancerous cells.[40] Indeed, we found: (1) no Slug-specific response element within the rat, mouse, or human *COX-2* gene, and (2) Slug is probably phosphorylated by ERK1/2 in VSMCs (the present study) and phosphorylated Slug, which is critical for *VIMENTIN* induction, does not directly bind the *VIMENTIN* promoter. As suggested for *VIMENTIN* gene upregulation mediated by Slug, *COX-2* gene upregulation probably involves additional transcription factors that are recruited by Slug in a Slug-phosphorylation–dependent manner.[40] In addition, the Slug-positive effect on *COX-2* is consistent with the Snail family implication in upregulating *COX-2* expression in oral keratinocytes.[44] The involvement of Slug in the PDGF-BB effect on the *COX-2* gene provides an explanation as to how PDGF-BB can induce the *COX-2* gene without activating nuclear factor κb–dependent signaling pathway in VSMCs.[54]

Our in vivo results demonstrate the existence of Slug-expressing cells in the neointima of human atherosclerotic plaques surrounding the lipid core (Figure 1), among which some are positive for the macrophage marker CD68, negative for SMA, and positive for smooth muscle–specific myosin heavy chain, respectively, early and late marker of SMC differentiation.[55] There is extensive evidence that SMCs within atherosclerotic lesions lack detectable expression of conventional SMC markers such as SMA and turn on the expression of macrophages markers.[56] In addition, human macrophages, activated or not, do not express any Slug transcript conversely to human VSMCs where Slug transcript and protein are well detected (Figures 2A and 3A). Based on these results, our in vitro results, and the literature, we conclude that neointimal Slug-expressing cells are most likely VSMCs that have adopted a macrophage-like phenotype and secrete PGE2, therefore contributing to plaque rupture and thrombogenicity. Based on the fact that Snail1 also promotes tumor progression and metastasis through an increase in PGE2 level,[57] Snail-dependent PGE2 secretion would be involved in life-threatening complications of both cancer and atherosclerosis.

Ox-LDL, one the main risk factors of atherosclerosis, has been shown to stabilize Snail1 in endothelial cells.[58] Here, we show that ox-LDLs synergize with PDGF-BB to increase Slug level and possibly Slug activity (Figure S7). Studies show that ox-LDLs triggering atherogenesis also cause cell transformation towards a malignancy status. This would be caused, at least in part, by their high density of the LOX-1 receptor.[59] Altogether, this suggests that the ox-LDL–induced cells showing partial transformation with some tumor-typical aspects is a Snail1/2-dependent phenomenon and defines Snail1/2 as a possible molecular connection between cardiovascular diseases and cancers. This hypothesis would provide a molecular explanation to the relationship between a high level of ox-LDL and cancer and reinforce the idea that controlling cholesterolemia and oxidative stress prevents both cardiovascular diseases and cancer.

Conclusions

Our results support a causal relationship between Slug and atherogenesis and propose a new role of Slug in plaque vulnerability and thrombogenicity, which is the cause of the acute clinical complications of atherosclerosis. This further emphasizes the already suggested roles of Snail1/2 in atherosclerosis where they would drive endothelial-mesenchymal transition, leading to plaque calcification, endothelial permeability, and plaque vulnerability.[60] Our results demonstrating a PDGF-BB/Slug-dependent change of phenotype of VSMC towards an inflammatory status renew the interest in PDGFs and their receptors as possible targets in treating atherosclerosis.[61] Imatinib, which selectively inhibits tyrosine kinase activity of PDGF receptors, has been prescribed to treat patients with gastrointestinal stromal tumor and chronic eosinophilic leukemia. Imatinib may now be tested in cardiovascular diseases since in mice it reduced inflammation markers and increased plaque stability.[62]

Acknowledgments

We are grateful to Drs Wade (Durham, North Carolina) and Dhasarathy (Grand Forks, Noth Dakota) for providing the adenovirus delivering the hemagglutinin-human Slug, to Drs Habener and Stanojevic (Boston, MA) for providing their Slug antibody, and to Prof Karabina (INSERM U1077, SU, Paris) who provided human macrophages.

Sources of Funding

This work was supported by Sorbonne Université and the Centre National de la Recherche Scientifique (CNRS).

Disclosures

None.

References

1. Libby P, Ridker PM, Hansson GK. Progress and challenges in translating the biology of atherosclerosis. *Nature*. 2011;473:317–325.
2. Bennett MR, Sinha S, Owens GK. Vascular smooth muscle cells in atherosclerosis. *Circ Res*. 2016;118:692–702.
3. Frontini MJ, O'Neil C, Sawyez C, Chan BMC, Huff MW, Pickering JG. Lipid incorporation inhibits Src-dependent assembly of fibronectin and type I collagen by vascular smooth muscle cells. *Circ Res*. 2009;104:832–841.
4. Nieto MA, Huang RY, Jackson RA, Thiery JP. EMT: 2016. *Cell*. 2016;166:21–45.
5. Newkirk KM, Duncan FJ, Brannick EM, Chandler HL, Parent AE, Kusewitt DF. The acute cutaneous inflammatory response is attenuated in Slug-knockout mice. *Lab Invest*. 2008;88:831–841.
6. Shirley SH, Grimm EA, Kusewitt DF. Ultraviolet radiation and the slug transcription factor induce proinflammatory and immunomodulatory mediator expression in melanocytes. *J Skin Cancer*. 2012;2012:410925.
7. Storci G, Bertoni S, De Carolis S, Papi A, Nati M, Ceccarelli C, Pirazzini C, Garagnani P, Ferrarini A, Buson G, Delledonne M, Fiorentino M, Capizzi E, Gruppioni E, Taffurelli M, Santini D, Franceschi C, Bandini G, Bonifazi F, Bonafé M. Slug/β-catenin–dependent proinflammatory phenotype in hypoxic breast cancer stem cells. *Am J Pathol*. 2013;183:1688–1697.
8. Shirley SH, Rundhaug JE, Perez CJ, Coletta LD, Kusewitt DF. Slug modulates UV radiation-induced cutaneous inflammation by regulating epidermal production of proinflammatory cytokines. *J Invest Dermatol*. 2017;137:532–534.
9. Ross R, Masuda J, Raines EW, Gown AM, Katsuda S, Sasahara M, Malden LT, Masuko H, Sato H. Localization of PDGF-B protein in macrophages in all phases of atherogenesis. *Science*. 1990;248:1009–1012.
10. Andrae J, Gallini R, Betsholtz C. Role of platelet-derived growth factors in physiology and medicine. *Genes Dev*. 2008;22:1276–1312.
11. He C, Medley SC, Hu T, Hinsdale ME, Lupu F, Virmani R, Olson LE. PDGFRβ signalling regulates local inflammation and synergizes with hypercholesterolaemia to promote atherosclerosis. *Nat Commun*. 2015;6:7770.
12. Xu K, Kitchen CM, Shu HK, Murphy TJ. Platelet-derived growth factor-induced stabilization of cyclooxygenase 2 mRNA in rat smooth muscle cells requires the c-Src family of protein-tyrosine kinases. *J Biol Chem*. 2007;282:32699–32709.
13. Bond M, Fabunmi RP, Baker AH, Newby AC. Synergistic upregulation of metalloproteinase-9 by growth factors and inflammatory cytokines: an absolute requirement for transcription factor NF-kappa B. *FEBS Lett*. 1998;435:29–34.
14. Cipollone F, Cicolini G, Bucci M. Cyclooxygenase and prostaglandin synthases in atherosclerosis: recent insights and future perspectives. *Pharmacol Ther*. 2008;118:161–180.
15. Libby P. Collagenases and cracks in the plaque. *J Clin Invest*. 2013;123:3201–3203.
16. Gross S, Tilly P, Hentsch D, Vonesch JL, Fabre JE. Vascular wall-produced prostaglandin E2 exacerbates arterial thrombosis and atherothrombosis through platelet EP3 receptors. *J Exp Med*. 2007;204:311–320.
17. Inaba T, Gotoda T, Shimano H, Shimada M, Harada K, Kozaki K, Watanabe Y, Hoh E, Motoyoshi K, Yazaki Y. Platelet-derived growth factor induces c-fms and scavenger receptor genes in vascular smooth muscle cells. *J Biol Chem*. 1992;267:13107–13112.
18. Rowe RG, Li XY, Hu Y, Saunders TL, Virtanen I, Garcia de Herreros A, Becker KF, Ingvarsen S, Engelholm LH, Bommer GT, Fearon ER, Weiss SJ. Mesenchymal cells reactivate Snail1 expression to drive three-dimensional invasion programs. *J Cell Biol*. 2009;184:399–408.
19. Kong D, Li Y, Wang Z, Banerjee S, Ahmad A, Kim HR, Sarkar FH. miR-200 regulates PDGF-D-mediated epithelial-mesenchymal transition, adhesion, and invasion of prostate cancer cells. *Stem Cells*. 2009;27:1712–1721.
20. Lu C, Sun X, Sun L, Sun J, Lu Y, Yu X, Zhou L, Gao X. Snail mediates PDGF-BB-induced invasion of rat bone marrow mesenchymal stem cells in 3D collagen and chick chorioallantoic membrane. *J Cell Physiol*. 2013;228:1827–1833.
21. Liu T, Ma W, Xu H, Huang M, Zhang D, He Z, Zhang L, Brem S, O'Rourke DM, Gong Y, Mou Y, Zhang Z, Fan Y. PDGF-mediated mesenchymal transformation renders endothelial resistance to anti-VEGF treatment in glioblastoma. *Nat Commun*. 2018;9:3439.
22. Tapia-Vieyra JV, Delgado-Coello B, Mas-Oliva J. Atherosclerosis and cancer; a resemblance with far-reaching implications. *Arch Med Res*. 2017;48:12–26.
23. Galle J, Wanner C. Oxidized LDL and Lp(a). Preparation, modification, and analysis. *Methods Mol Biol*. 1998;108:119–130.
24. Keuylian Z, de Baaij JHF, Glorian M, Rouxel C, Merlet E, Lipskaia L, Blaise R, Mateo V, Limon I. The Notch pathway attenuates interleukin 1 (IL1)-mediated induction of adenylyl cyclase 8 (AC8) expression during vascular smooth muscle cell (VSMC) trans-differentiation. *J Biol Chem*. 2012;287:24978–24989.
25. Jumeau C, Awad F, Assrawi E, Cobret L, Duquesnoy P, Giurgea I, Valeyre D, Grateau G, Amselem S, Bernaudin JF, Karabina SA. Expression of SAA1, SAA2 and SAA4 genes in human primary monocytes and monocyte-derived macrophages. *PLoS One*. 2019;14:e0217005.
26. Dhasarathy A, Phadke D, Mav D, Shah RR, Wade PA. The transcription factors snail and slug activate the transforming growth factor-beta signaling pathway in breast cancer. *PLoS One*. 2011;6:e26514.
27. Gueguen M, Keuylian Z, Mateo V, Mougenot N, Lompré AM, Michel JB, Meilhac O, Lipskaia L, Limon I. Implication of adenylyl cyclase 8 in pathological smooth muscle cell migration occurring in rat and human vascular remodelling. *J Pathol*. 2010;221:331–342.
28. Blirando K, Blaise R, Gorodnaya N, Rouxel C, Meilhac O, Vincent P, Limon I. The stellate vascular smooth muscle cell phenotype is induced by IL-1β via the secretion of PGE2 and subsequent cAMP-dependent protein kinase A activation. *Biochim Biophys Acta*. 2015;1853:3235–3247.
29. Stary HC, Chandler AB, Dinsmore RE, Fuster V, Glagov S, Insull W, Rosenfeld ME, Schwartz CJ, Wagner WD, Wissler RW. A definition of advanced types of atherosclerotic lesions and a histological classification of atherosclerosis. A report from the Committee on Vascular Lesions of the Council on Arteriosclerosis, American Heart Association. *Arterioscler Thromb Vasc Biol*. 1995;15:1512–1531.
30. Phan-Hug F, Guimiot F, Lelièvre V, Delezoide AL, Czernichow P, Breant B, Blondeau B. Potential role of glucocorticoid signaling in the formation of pancreatic islets in the human fetus. *Pediatr Res*. 2008;64:346–351.
31. Rukstalis JM, Habener JF. Snail2, a mediator of epithelial-mesenchymal transitions, expressed in progenitor cells of the developing endocrine pancreas. *Gene Expr Patterns*. 2007;7:471–479.
32. Shankman LS, Gomez D, Cherepanova OA, Salmon M, Alencar GF, Haskins RM, Swiatlowska P, Newman AAC, Greene ES, Straub AC, Isakson B, Randolph GJ, Owens GK. KLF4-dependent phenotypic modulation of smooth muscle cells has a key role in atherosclerotic plaque pathogenesis. *Nat Med*. 2015;21:628–637.
33. Vengrenyuk Y, Nishi H, Long X, Ouimet M, Savji N, Martinez FO, Cassella CP, Moore KJ, Ramsey SA, Miano JM, Fisher EA. Cholesterol loading reprograms the microRNA-143/145-myocardin axis to convert aortic smooth muscle cells to a dysfunctional macrophage-like phenotype. *Arterioscler Thromb Vasc Biol*. 2015;35:535–546.
34. Miano JM, Cserjesi P, Ligon KL, Periasamy M, Olson EN. Smooth muscle myosin heavy chain exclusively marks the smooth muscle lineage during mouse embryogenesis. *Circ Res*. 1994;75:803–812.
35. Zhou BP, Deng J, Xia W, Xu J, Li YM, Gunduz M, Hung M-C. Dual regulation of Snail by GSK-3beta-mediated phosphorylation in control of epithelial-mesenchymal transition. *Nat Cell Biol*. 2004;6:931–940.
36. Wu ZQ, Li XY, Hu CY, Ford M, Kleer CG, Weiss SJ. Canonical Wnt signaling regulates Slug activity and links epithelial-mesenchymal transition with epigenetic Breast Cancer 1, Early Onset (BRCA1) repression. *Proc Natl Acad Sci USA*. 2012;109:16654–16659.

37. Kim JY, Kim YM, Yang CH, Cho SK, Lee JW, Cho M. Functional regulation of Slug/Snail2 is dependent on GSK-3β-mediated phosphorylation. *FEBS J*. 2012;279:2929–2939.
38. Kao SH, Wang WL, Chen CY, Chang YL, Wu YY, Wang YT, Wang SP, Nesvizhskii AI, Chen YJ, Hong TM, Yang PC. GSK3β controls epithelial-mesenchymal transition and tumor metastasis by CHIP-mediated degradation of Slug. *Oncogene*. 2014;33:3172–3182.
39. Sklepkiewicz P, Schermuly RT, Tian X, Ghofrani HA, Weissmann N, Sedding D, Kashour T, Seeger W, Grimminger F, Pullamsetti SS. Glycogen synthase kinase 3beta contributes to proliferation of arterial smooth muscle cells in pulmonary hypertension. *PLoS One*. 2011;6:e18883.
40. Virtakoivu R, Mai A, Mattila E, De Franceschi N, Imanishi SY, Corthals G, Kaukonen R, Saari M, Cheng F, Torvaldson E, Kosma VM, Mannermaa A, Muharram G, Gilles C, Eriksson J, Soini Y, Lorens JB, Ivaska J. Vimentin-ERK signaling uncouples slug gene regulatory function. *Cancer Res*. 2015;75:2349–2362.
41. Cobaleda C, Pérez-Caro M, Vicente-Dueñas C, Sánchez-García I. Function of the zinc-finger transcription factor SNAI2 in cancer and development. *Annu Rev Genet*. 2007;41:41–61.
42. Esfandiarei M, Yazdi SA, Gray V, Dedhar S, van Breemen C. Integrin-linked kinase functions as a downstream signal of platelet-derived growth factor to regulate actin polymerization and vascular smooth muscle cell migration. *BMC Cell Biol*. 2010;11:16.
43. Robida AM, Xu K, Ellington ML, Murphy TJ. Cyclosporin A selectively inhibits mitogen-induced cyclooxygenase-2 gene transcription in vascular smooth muscle cells. *Mol Pharmacol*. 2000;58:701–708.
44. Lyons JG, Patel V, Roue NC, Fok SY, Soon LL, Halliday GM, Gutkind JS. Snail up-regulates proinflammatory mediators and inhibits differentiation in oral keratinocytes. *Cancer Res*. 2008;68:4525–4530.
45. Tall AR, Yvan-Charvet L, Terasaka N, Pagler T, Wang N. HDL, ABC transporters, and cholesterol efflux: implications for the treatment of atherosclerosis. *Cell Metab*. 2008;7:365–375.
46. Nagao S, Murao K, Imachi H, Cao WM, Yu X, Li J, Matsumoto K, Nishiuchi T, Ahmed RA, Wong NC, Ueda K, Ishida T. Platelet derived growth factor regulates ABCA1 expression in vascular smooth muscle cells. *FEBS Lett*. 2006;580:4371–4376.
47. Ding G, Fang J, Tong S, Qu L, Jiang H, Ding Q, Liu J. Over-expression of lipocalin 2 promotes cell migration and invasion through activating ERK signaling to increase SLUG expression in prostate cancer. *Prostate*. 2015;75:957–968.
48. Coll-Bonfill N, Peinado VI, Pisano MV, Párrizas M, Blanco I, Evers M, Engelmann JC, García-Lucio J, Tura-Ceide O, Meister G, Barberà JA, Musri MM. Slug is increased in vascular remodeling and induces a smooth muscle cell proliferative phenotype. *PLoS One*. 2016;11:e0159460.
49. Lacolley P, Regnault V, Segers P, Laurent S. Vascular smooth muscle cells and arterial stiffening: relevance in development, aging, and disease. *Physiol Rev*. 2017;97:1555–1617.
50. Yang S, Ye ZM, Chen S, Luo XY, Chen SL, Mao L, Li Y, Jin H, Yu C, Xiang FX, Xie MX, Chang J, Xia YP, Hu B. MicroRNA-23a-5p promotes atherosclerotic plaque progression and vulnerability by repressing ATP-binding cassette transporter A1/G1 in macrophages. *J Mol Cell Cardiol*. 2018;123:139–149.
51. Tedgui A, Mallat Z. Apoptosis as a determinant of atherothrombosis. *Thromb Haemost*. 2001;86:420–426.
52. Medici D, Kalluri R. Endothelial-mesenchymal transition and its contribution to the emergence of stem cell phenotype. *Semin Cancer Biol*. 2012;22:379–384.
53. Phillips S, Kuperwasser C. SLUG: critical regulator of epithelial cell identity in breast development and cancer. *Cell Adh Migr*. 2014;8:578–587.
54. Mehrhof FB, Schmidt-Ullrich R, Dietz R, Scheidereit C. Regulation of vascular smooth muscle cell proliferation: role of NF-kappaB revisited. *Circ Res*. 2005;96:958–964.
55. Gomez D, Swiatlowska P, Owens GK. Epigenetic control of smooth muscle cell identity and lineage memory. *Arterioscler Thromb Vasc Biol*. 2015;35:2508–2516.
56. Allahverdian S, Chaabane C, Boukais K, Francis GA, Bochaton-Piallat ML. Smooth muscle cell fate and plasticity in atherosclerosis. *Cardiovasc Res*. 2018;114:540–550.
57. Mann JR, Backlund MG, Buchanan FG, Daikoku T, Holla VR, Rosenberg DW, Dey SK, DuBois RN. Repression of prostaglandin dehydrogenase by epidermal growth factor and snail increases prostaglandin E2 and promotes cancer progression. *Cancer Res*. 2006;66:6649–6656.
58. Su Q, Sun Y, Ye Z, Yang H, Li L. Oxidized low density lipoprotein induces endothelial-to-mesenchymal transition by stabilizing Snail in human aortic endothelial cells. *Biomed Pharmacother*. 2018;106:1720–1726.
59. Balzan S, Lubrano V. LOX-1 receptor: a potential link in atherosclerosis and cancer. *Life Sci*. 2018;198:79–86.
60. Kovacic JC, Dimmeler S, Harvey RP, Finkel T, Aikawa E, Krenning G, Baker AH. Endothelial to mesenchymal transition in cardiovascular disease: JACC State-of-the-Art Review. *J Am Coll Cardiol*. 2019;73:190–209.
61. Hu W, Huang Y. Targeting the platelet-derived growth factor signalling in cardiovascular disease. *Clin Exp Pharmacol Physiol*. 2015;42:1221–1224.
62. Pouwer MG, Pieterman EJ, Verschuren L, Caspers MPM, Kluft C, Garcia RA, Aman J, Jukema JW, Princen HMG. The BCR-ABL1 inhibitors imatinib and ponatinib decrease plasma cholesterol and atherosclerosis, and nilotinib and ponatinib activate coagulation in a translational mouse model. *Front Cardiovasc Med*. 2018;5:55.

Supplemental Material

Table S1. List of compounds, cells, cell media and their sources .

Sigma-Aldrich	CHIR 99021, U 0126, LY 20004, phorbol 12-myristate 13 acetate (PMA), Dulbecco's Eagle Medium (DMEM), Bovine Serum Albumin (BSA), trypsin, tween 20, hematoxylin, lipofectamine RNAimax, glutamine, penicillin, streptomycin, paraformaldehyde (PFA), triton x 100, Nonidet P-40, 4′,6-Diamidine-2′-phenylindole dihydrochloride (DAPI), acrylamid, Sodium Dodecyl Sulfate (SDS), β–mercaptoethanol
Peprotech	Recombinant human PDGF-BB, IL1-β, TNF-α and INF-γ
Life Technologies	RPMI 1640 medium, fetal bovine serum (FBS), protease and phosphatase inhibitors, nitrocellulose membranes, ECL detection reagent, cell extraction buffer (CEB)
Enzo Life Sciences	PD 98059, MG 132
Lonza	Human Aortic Smooth Muscle Cells (AoSMC cells), Smooth Muscle Growth Medium 2 (SmGM-2), smooth muscle cell-specific growth factors and supplements, fetal bovine serum (FBS)
Dako	Fluorescence mounting medium, HRP substrate DAB (3-3' diaminobenzidine), glycergel
National Diagnostics	Histoclear
Eurogentec	siRNAs SLUG
Si TOOLs Biotech	siRNA control
MWG Eurofins	DNA oligonucleotides

Table S2. List of primers used for real-time PCR and siRNA experiments .

	Target gene	Forward primer (5'-3')	Reverse primer (5'-3')	Accession number
Real time PCR for mRNA relative quantification	Rat Snail1	gaagatgcacatccgaag	agtgggagcaggagaaag	NM_053805
	Rat Slug	gagctaccccatgcctgtc	agggctgtacgctcctga	NM_013035
	Rat COX-2	ggaagtctttggtctggt	tcttgatcgtctctcgtatcagta	NM_017232
	Rat ABCA1	gcctgttggtgatcatcttg	accacgctggggtcactat	NM_178095.2
	Rat ABCG1	gctgctgcctcacctcac	ccttcatccctctcttgcag	NM_053502.1
	Rat Cyclophilllin A	tgctggaccaaacacaaatg	cttcccaaagaccacatgct	NM_017101
	Human Slug	ccatgcctgtcataccacaa	acagtgatggggctgtatgc	NM_003068.4
	Human Snail1	gctgcaggactctaatccaga	atctccggaggtgggatg	NM_005985.3
	Human interleukin 1-β	acacatgggataacgagg	atggaccagacatcaccaa	NM_000576.3
	Human MCP-1	agtctctgccgcccttct	gtgactggggcattgattg	NM_002982.4
	Human CXCL-10	gaaagcagttagcaaggaaaggt	gacatatactccatgtagggaagtga	NM_001565.4
	Human HPRT	tgtaatgaccagtcaacaggg	ccagtgtcaattatatcttccacaatc	NM_000194

	siRNA denomination	Forward primer (5'-3')	Reverse primer (5'-3')
siRNA	siSlug-1	gcugagaaguuucagugcaauuuautt	auaaauugcacugaaacuucucagctt
	siSlug-2	ccucuuacuggauacuccucaucuuutt	aagaugaggaguauccaguaagaggtt
	siSlug-3	ccacucugauguaaagaaatt	uuucuuuacaucagaguggtt

Table S3. List of antibodies used in immunoblots, immunofluorescence and immunochemistry experiments.

Primary antibodies

Target protein	Sources	Manufacturers	Catalog numbers
Ha-Tag	Mouse monoclonal	Abcam	ab130275
Phospho-GSK3-b (Ser9)	Rabbit monoclonal	Cell Signaling	9322
Akt	Rabbit polyclonal	Cell Signaling	9272
Phospho-Akt (Ser473)	Rabbit monoclonal	Cell Signaling	4060
p44/42 MAPK (Erk1/2)	Rabbit monoclonal	Cell Signaling	4695
Phospho-p44/42 MAPK (Erk1/2) (Thr 202/Tyr 204)	Rabbit monoclonal	Cell Signaling	4370
HDAC-1	Mouse monoclonal	Santa Cruz	sc-81598
COX-2	Rabbit polyclonal	Abcam	ab15191
GAPDH	Rabbit monoclonal	Abcam	ab181602
Slug, antibody # 1	Rabbit polyclonal	Gift from Habener's lab	_
Slug, antibody # 2	Rabbit monoclonal	Cell Signaling	9585
SMA	Mouse monoclonal	Dako	M0851
CD68	Mouse monoclonal	Dako	M0814
SMMHC	Rabbit polyclonnal	Sigma-Aldrich	HPA015310

Secondary antibodies

Target protein and conjugate	Sources	Manufacturers	Catalog numbers
Mouse IgG(H+L)-HRP	Goat polyclonal	Abliance	BI 2413-C
Rabbit IgG(H+L)-HRP	Goat polyclonal	Abliance	BI 2407
Mouse IgG(H+L)-Alexa fluor 594	Donkey polyclonal	Life Technologies	A 21203

Supplemental Figure Legends:

Figure S1. Slug is expressed principally in vascular smooth muscle cells that adopted a macrophage-like phenotype in the neointima of type VI atherosclerotic lesions of human carotid arteries. Serial sections of a representative human type VI atherosclerotic lesion obtained from a carotid endarterectomy sample counterstained with hematoxylin and immunolabeled with an anti-Slug, an anti-CD68 or an anti-SMMHC. Images of right panels are obtained at magnification x 10 Proteins of interest appearing in brown are indicated by black arrows. Cholesterol clefts are indicated by red arrows. The images are representative of serial sections from 4 different patients. a, adventitia, m, media; * lipid core; ** fibrous cap; l, lumen, ns non specific labelling.

Figure S2. Snail1 transcripts are expressed by human macrophages and aortic smooth muscle cells. Primary human macrophages and primary human aortic smooth muscle cells (AoSMC) were rendered quiescent by serum deprivation. Snail1 mRNA expression was assessed by RT-qPCR. PCR results are expressed the mean relative ratio (*SNAI1* gene /reference gene *HPRT*) obtained from 4 independent experiments.

Figure S3. Densitometry analysis of Slug level in Figure 4, panels A and B. Results are normalized relative to GAPDH and expressed as the fold relative to vehicle-treated cells. Bars represent the mean ± SEM of 4 independent experiments. *, $p < 0.05$. PDFG-BB *vs* PDGF-BB+MG132 treated cells, ns: not significant.

Figure S4. Specificity and efficiency of Slug siRNA. A. Relative slug mRNA expression (RT-qPCR) in VSMC transfected with control or Slug siRNA. **B.** Snail 1 and Snail 3 mRNA expression in control (ctl) and Slug siRNA transfected cells. Results are normalized relative to cyclophilin A (cycloA) mRNA levels and expressed as the fold relative to VSMC transfected with control siRNA. Bars represent the mean ± SEM of 6 independent experiments. **, $p < 0.005$, ns: not significant.

Figure S5. PDGF-BB allows rat VSMCs to secrete PGE2. Rat aortic smooth muscle cells (rat VSMCs) were treated or not during 9 hours with PDGF-BB (10ng/ml). PGE2 concentrations in cell supernatant were determined. Values represent the mean ± SEM of 4 independent experiments. *, $p < 0.05$.

Figure S6. PDGF-BB triggers Oxidized LDLs uptake in human VSMCs. A. Snapshots of Dil-labeled-ox-LDL (Dil-ox-LDL, 10 µg/ml, 4h) uptake by vehicle- or PDGF-BB- (10 ng/ml, 24 h) treated cells. Cells are fixed with PFA and DAPI-stained. Uptake was analyzed by fluorescence microscopy (20x). Images shown are representative of 3 independent experiments where six different fields per condition were examined. **B.** Flow cytometry histogram showing PDGF-BB-mediated positive effect on Dil-oxLDL uptake.

Figure S7. Oxidized LDLs and PDGF-BB synergize to induce Slug expression in rat VSMCs. Upper panel: Representative western blot showing the effect of PDGF-BB (2 and 10 ng/ml) and oxidized LDL (oxLDL, 50 µg/ml) alone or combined on Ha-Slug protein expression in rat VSMCs overexpressing human Slug-HA The western images are representative from 4 independent experiments. **Lower panel**: Quantification of the bands intensity. Results are normalized relative to GAPDH and expressed as the mean fold over untreated VSMCs. *, $p < 0.05$

Figure S1

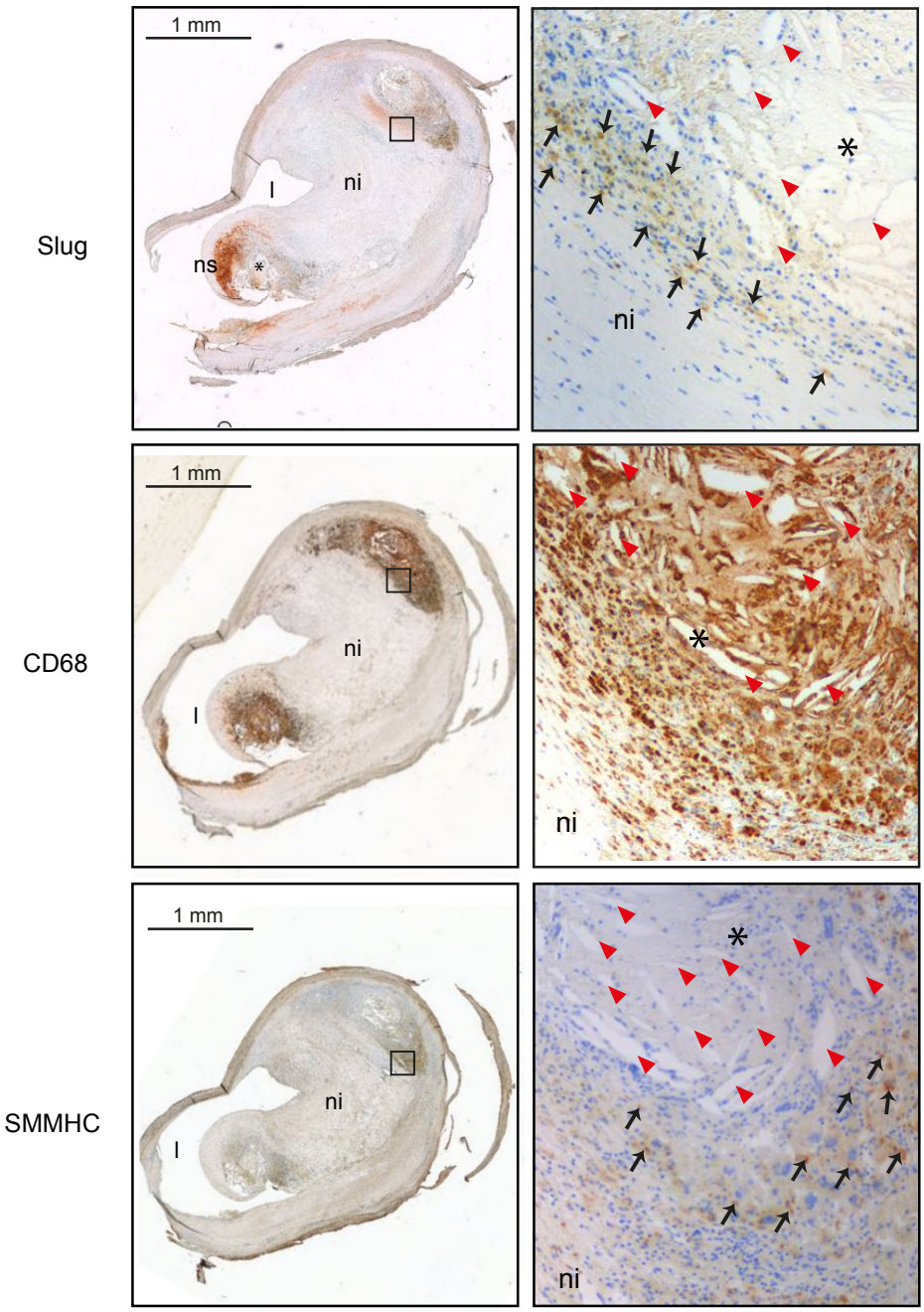

Figure S2

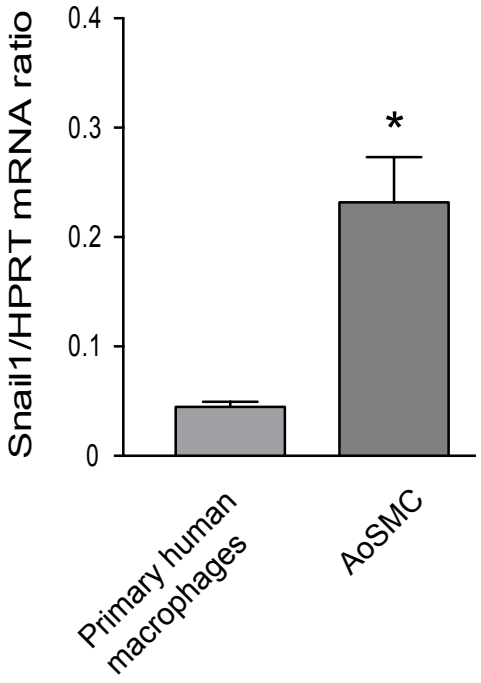

Figure S3

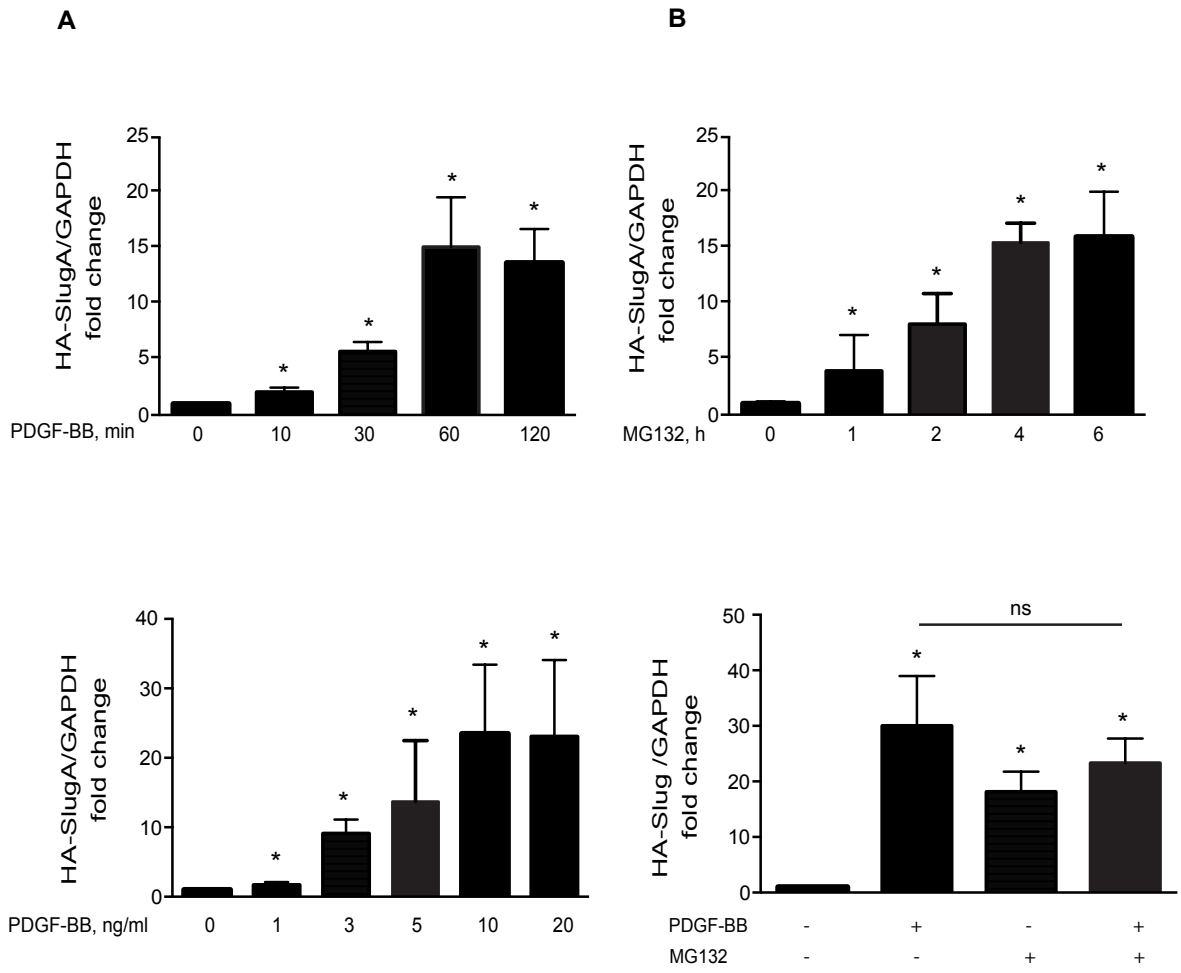

Figure S4

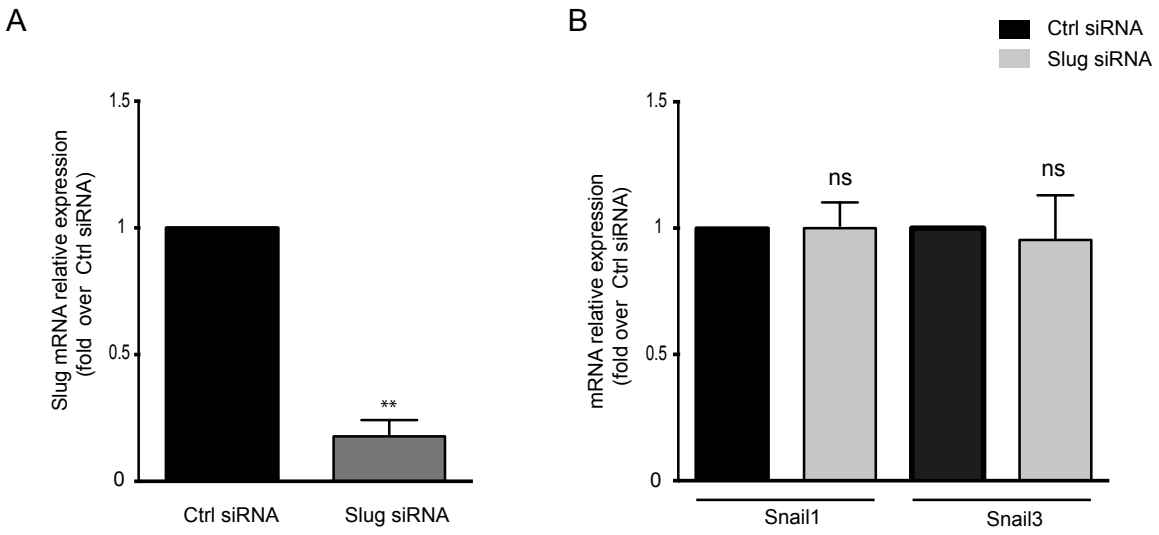

Figure S5

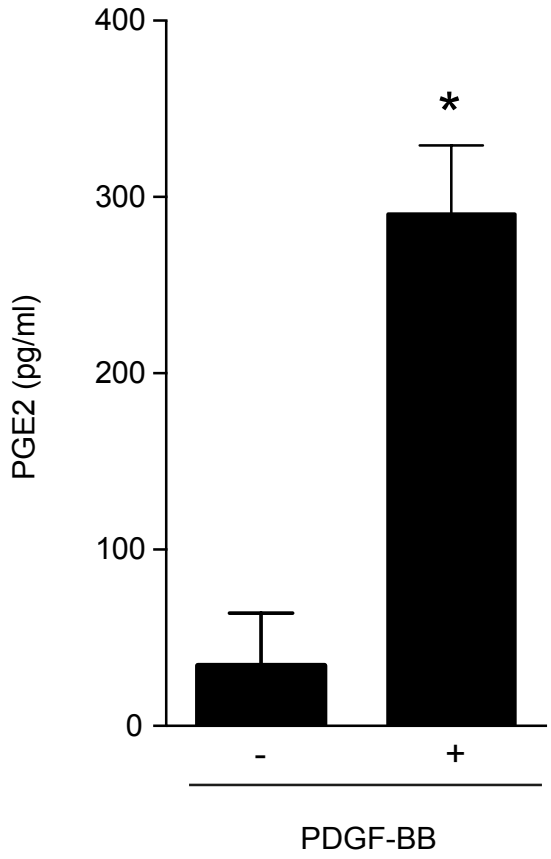

Figure S6

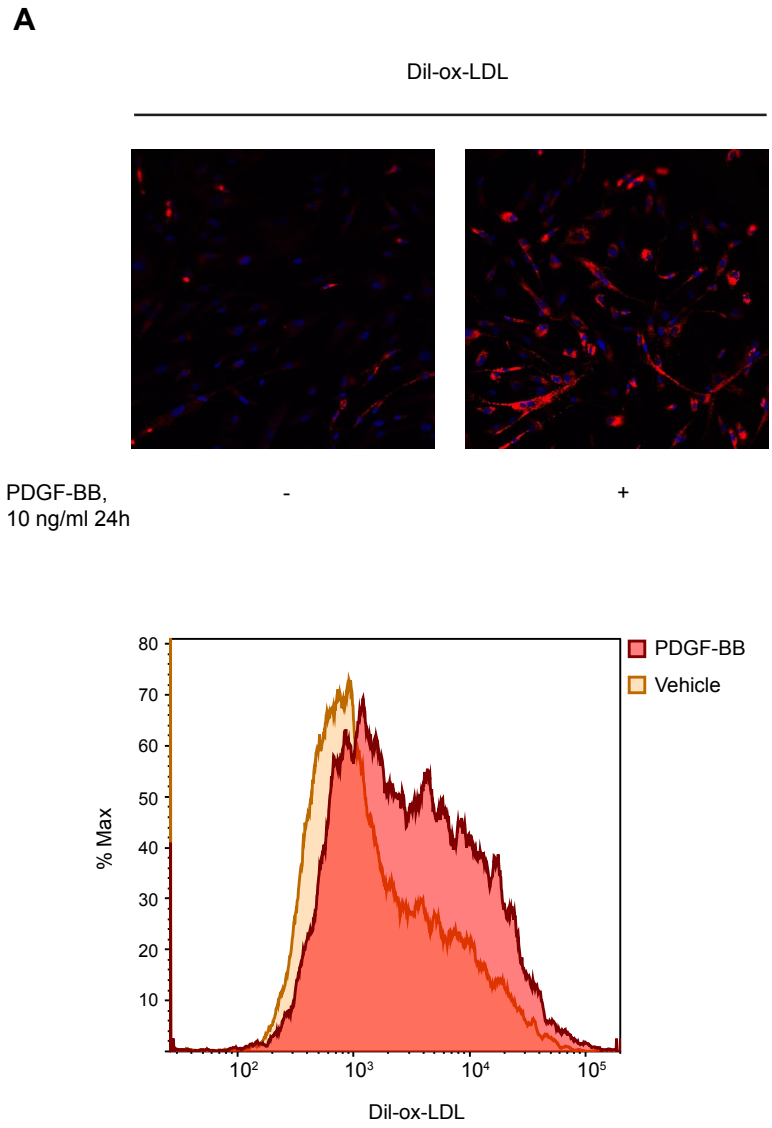

Figure S7